NASA/TP-2006-213729

Reach Envelope and Field of Vision Quantification in Mark III Space Suit using Delaunay Triangulation

Andrew F. J. Abercromby
Sherry S. Thaxton
Elizabeth A. Onady
Sudhakar L. Rajulu

November 2006

The NASA STI Program Office ... in Profile

Since its founding, NASA has been dedicated to the advancement of aeronautics and space science. The NASA Scientific and Technical Information (STI) Program Office plays a key part in helping NASA maintain this important role.

The NASA STI Program Office is operated by Langley Research Center, the lead center for NASA's scientific and technical information. The NASA STI Program Office provides access to the NASA STI Database, the largest collection of aeronautical and space science STI in the world. The Program Office is also NASA's institutional mechanism for disseminating the results of its research and development activities. These results are published by NASA in the NASA STI Report Series, which includes the following report types:

- TECHNICAL PUBLICATION. Reports of completed research or a major significant phase of research that present the results of NASA programs and include extensive data or theoretical analysis. Includes compilations of significant scientific and technical data and information deemed to be of continuing reference value. NASA counterpart of peer-reviewed formal professional papers, but having less stringent limitations on manuscript length and extent of graphic presentations.
- TECHNICAL MEMORANDUM. Scientific and technical findings that are preliminary or of specialized interest, e.g., quick release reports, working papers, and bibliographies that contain minimal annotation. Does not contain extensive analysis.
- CONTRACTOR REPORT. Scientific and technical findings by NASA-sponsored contractors and grantees.
- CONFERENCE PUBLICATION. Collected papers from scientific and technical conferences, symposia, seminars, or other meetings sponsored or co-sponsored by NASA.
- SPECIAL PUBLICATION. Scientific, technical, or historical information from NASA programs, projects, and missions, often concerned with subjects having substantial public interest.
- TECHNICAL TRANSLATION. English-language translations of foreign scientific and technical material pertinent to NASA's mission.

Specialized services that complement the STI Program Office's diverse offerings include creating custom thesauri, building customized databases, organizing and publishing research results ... even providing videos.

For more information about the NASA STI Program Office, see the following:

- Access the NASA STI Program Home Page at ***http://www.sti.nasa.gov***
- E-mail your question via the Internet to help@sti.nasa.gov
- Fax your question to the NASA STI Help Desk at (301) 621-0134
- Telephone the NASA STI Help Desk at (301) 621-0390
- Write to:
  NASA STI Help Desk
  NASA Center for AeroSpace Information
  7121 Standard Drive
  Hanover, MD 21076-1320

NASA/TP—2006–213729

Reach Envelope and Field of Vision Quantification in Mark III Space Suit using Delaunay Triangulation

Andrew F. J. Abercromby
MEI Technologies, Inc.
Houston, TX

Sherry S. Thaxton
Lockheed Martin.
Houston, TX

Elizabeth A. Onady
LZ Tech
Houston, TX

Sudhakar L. Rajulu
NASA, Johnson Space Center
Houston, TX

National Aeronautics and
Space Administration

Lyndon B. Johnson Space Center
Houston, Texas 77058

November 2006

CONTENTS

Available from:

NASA Center for AeroSpace Information
7121 Standard Drive
Hanover, MD 21076-1320
301-621-0390

National Technical Information Service
5285 Port Royal Road
Springfield, VA 22161
703-605-6000

This report is also available in electronic form at http://techreports.larc.nasa.gov/cgi-bin/NTRS

TABLES

FIGURES

ACRONYMS

ABF	Anthropometry and Biomechanics Facility
EVA	Extra Vehicular Activity
FOV	Field of Vision
HSIR	Human Systems Integration Requirements
HUT	Hard Upper Torso
NSTS	National Space Transportation System
PFR	Portable Foot Restraint
PLSS	Primary Life Support System
RMS	Root Mean Square
S1	Subject 1
S2	Subject 2
SCOUT	Science Crew Operations and Utility Testbed
2-D	Two-dimensional
3-D	Three-dimensional

1. INTRODUCTION

The Science Crew Operations and Utility Testbed (SCOUT) project is focused on the development of a rover vehicle that can be utilized by two crewmembers during extra vehicular activities (EVAs) on the moon and Mars. The current SCOUT vehicle can transport two suited astronauts riding in open cockpit seats. Among the aspects currently being developed is the cockpit design and layout. This process includes the identification of possible locations for a socket to which a crewmember could connect a portable life support system (PLSS) for recharging power, air, and cooling while seated in the vehicle. The spaces in which controls and connectors may be situated within the vehicle are constrained by the reach and vision capabilities of the suited crewmembers. Accordingly, quantification of the volumes within which suited crewmembers can both see and reach relative to the vehicle represents important information during the design process.

The Mark III space suit (Figure 1) is a prototype suit being developed for EVAs on the moon and Mars. The suit includes a hard upper torso (HUT), brief and hip transition elements, rolling convolute shoulder, and waist and hip abduction/adduction joints; and also incorporates upper arm, shoulder, hip, waist, and ankle bearings. All spacesuits restrict the movements of the crewmember wearing the suit to some extent. The mechanical constraints, weight, and the pressurization of each space suit act to reduce or eliminate certain degrees of freedom that are available during normal unsuited human motion. The ease, efficiency, and effectiveness with which movements or tasks can be performed in a specific space suit are a result of the extent to which that suit reduces the ranges of motion in the various joints of that suit. Among the most basic and most important movements is reaching with the arms and hands, which is a prerequisite to performing almost any other task. Accordingly, reach evaluation is an essential ergonomic consideration when designing a space suit and any interfaces between a subject wearing that space suit and other hardware.

The reach envelope for any space suit differs according to the anthropometry and strength of the person wearing the suit. The maximum reach envelopes for 5^{th} and 95^{th} percentile males in the extravehicular mobility unit (EMU) while attached to the portable foot restraint (PFR) are defined in NSTS 07700 (1). However, data on the inner bounds of the reach envelopes are not provided. No quantitative information is currently available regarding the reach envelope for the Mark III suit under any conditions.

Reach envelopes may be determined numerically by quantifying the individual ranges of motion in each joint and then using forward kinematics to computationally determine all possible locations of the hand. However, the joint ranges of motion are not necessarily independent from each other. A numerically-derived solution for the reach envelope may not yield an accurate estimate for the actual reach envelope. Nor does it incorporate an individual's strength characteristics unless joint torque data is also used. Until a numerical approach to quantifying suited reach envelopes can be validated, the only reliable method to quantify reach envelopes is to empirically collect position data from each hand during a comprehensive series of reaching motions.

Field of vision (FOV) data is also important in human-machine interface design; for operations such as PLSS recharging, controls must be positioned such that the crewmember can both reach and see the connection. Indeed, the work envelope can be defined as the volume within which a crewmember can both see and comfortably reach (2).

This study was intended as a preliminary assessment of the reach envelope and field of vision of suited subjects as it relates to designing the human-machine interfaces on the rover. By quantifying the reach envelopes of suited crewmembers, suit and rover interfaces can be designed to ensure that all members of the crew population can be accommodated. The specific objectives of this study were:

- To quantitatively determine the volume (or 'envelope') within which a suited crewmember could reach when attempting to connect the PLSS on their pressurized Mark III EVA suit to the SCOUT vehicle for recharge.
- To quantitatively determine the FOV in the lateral and vertical directions for suited and unsuited subjects.

In this study, the reach envelopes and FOV of two suited and unsuited subjects were empirically evaluated while seated in the SCOUT vehicle using 3-dimensional position data collected during a series of reaching motions. Data were collected in laboratory (indoor) and field (outdoor) conditions. An analysis procedure was developed specifically for this task wherein data were interpolated and displayed in orthogonal views and in 100mm cross-sections. The data processing and analysis techniques developed for this project are potentially applicable in the evaluation of other human-machine interfaces such as spacecraft cockpits.

2. METHODS

2.1 STUDY DESIGN

Reach and vision data were collected from two seated male subjects (Table 1) during laboratory testing. One of the two subjects also participated in field testing, the purpose of which was to cross-validate the laboratory data with data collected in a more realistic operational environment. The anthropometric percentile characteristics of the subjects were determined using the Human Systems Integration Requirements (HSIR) document. This requirements document uses 2015 projected anthropometric data to ensure future crewmembers are adequately represented for design considerations.

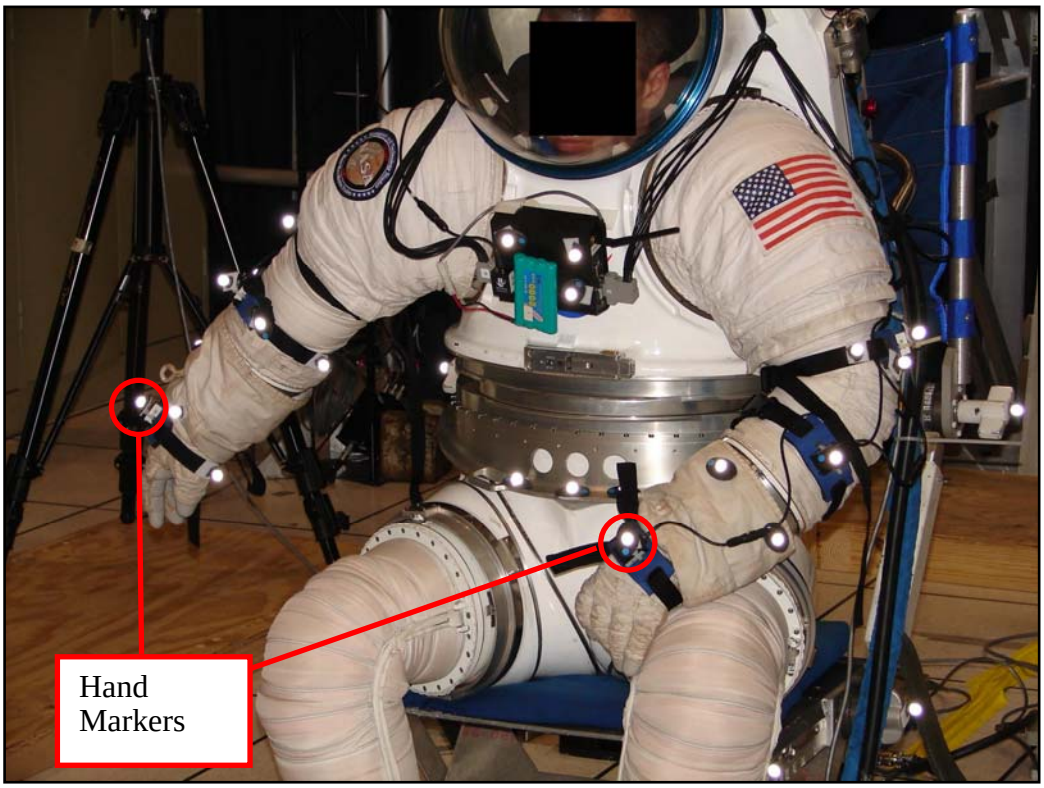

Figure 1. Suited subject wearing Mark III EVA suit and retro-reflective tracking markers during laboratory data collection.

Table 1. Subject height, weight, and strength information.

	Stature (cm)	Weight (kg)	Stature as Percentile of Projected 2015 Astronaut Population	Upper Body Strength as Percentile of Current Astronaut Population
Subject 1	188.9	99.0	94%	79%
Subject 2	178.5	70.2	49%	91%

During laboratory testing, the reach and vision capabilities of each subject were evaluated while sitting in shirtsleeve unsuited conditions and while wearing a pressurized Mark III

space suit. The two conditions enabled comparison of the suited reach envelope and vision capabilities with the 'normal' unsuited capabilities for each subject. Subjects sat on the Blue Static Seat with the Blue Cushion (Figure 1).

During field testing, reach and vision were evaluated only during suited conditions. While wearing the same Mark III suit Subject 1 sat in the left side molded seat of the SCOUT vehicle with the Mark III seat cushion. The rover was stationary on level grassy terrain. No noticeable movement of the hard upper torso (HUT) occurred during laboratory or field testing. The seats, and the cushions on the seats, differed between laboratory and field testing conditions, as discussed in Section 4.

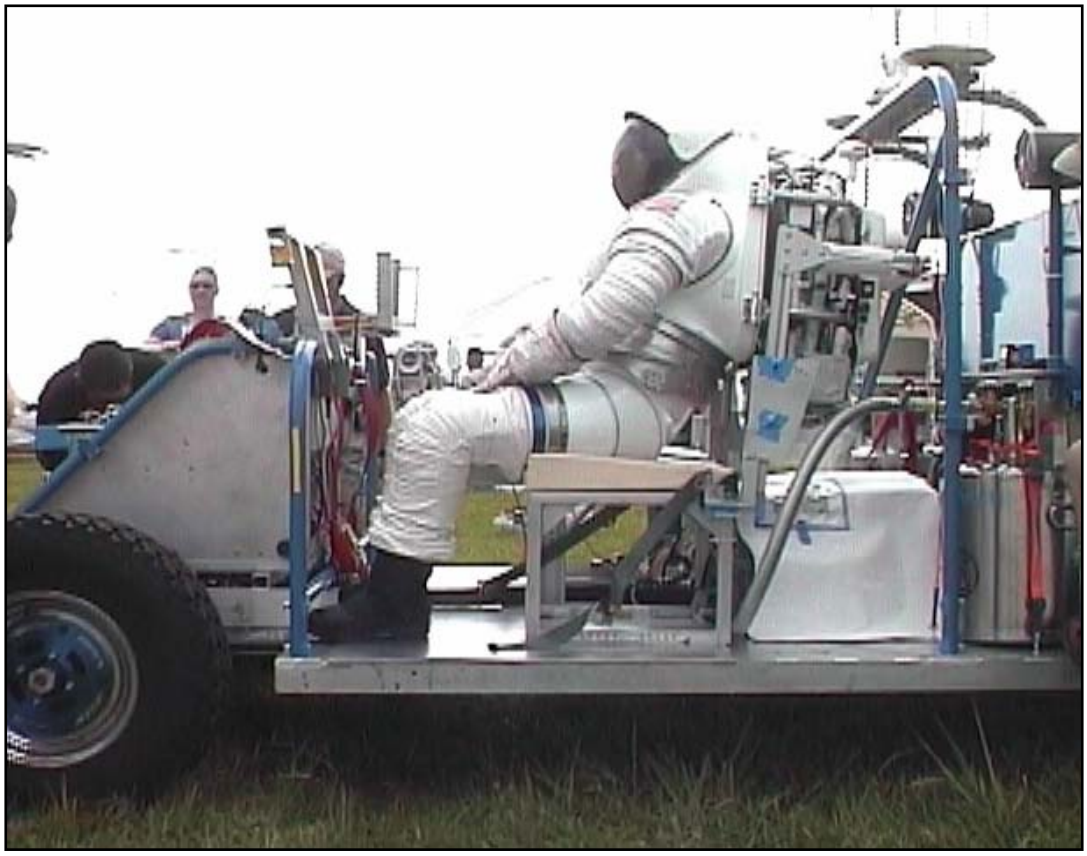

Figure 2. Suited subject wearing Mark III EVA suit during field data collection.

2.2 REACH MEASUREMENT

Laboratory Testing

A 10-camera Vicon 612 motion capture system (Vicon Peak, Oxford, United Kingdom) running Vicon iQ software version 2.5 was used to collect 3-dimensional (3-D) position data (Sampling Rate: 200Hz; RMS error < ±1mm) from retro-reflective markers attached to the back of each hand. Markers were attached to the dorsal side of each hand or glove over the midpoint of the third metacarpal (Figure 1). By defining the reach envelope as the volume within which the middle of the hand could be positioned by the subject, it may be inferred that any object within the reach volume of each hand may be grasped by the fingers. Markers were also attached to the corners of the chair and to each subject's

chest. The origin of the coordinate system was the midpoint of the front edge of the seat pan. Additional motion tracking devices and retro-reflective markers were attached to the subject for the purpose of an unrelated evaluation of a gyroscope-based motion tracking device. The additional equipment had negligible mass and did not interfere with subjects' reach.

During the shirtsleeve and suited trials, subjects were instructed by a test operator to move their right hand through a series of lateral and vertical arm-hand motions (Figure 3), which defined the inner and outer boundaries of the reach envelope for the right hand. The process was then repeated for the left hand.

It was impracticable to have subjects fully define the entirety of their reach envelopes by moving their hands in every possible 3-D location because of the excessive time that would be required and the unavailability of real-time data visualization. The 3-D position data from each hand were analyzed with a custom program using MATLAB 7 (The MathWorks, Inc., Natick, Maryland). The unprocessed position data collected from the chair corners and from the left and right hands of Subject 2 during suited trials are shown in Figure 4.

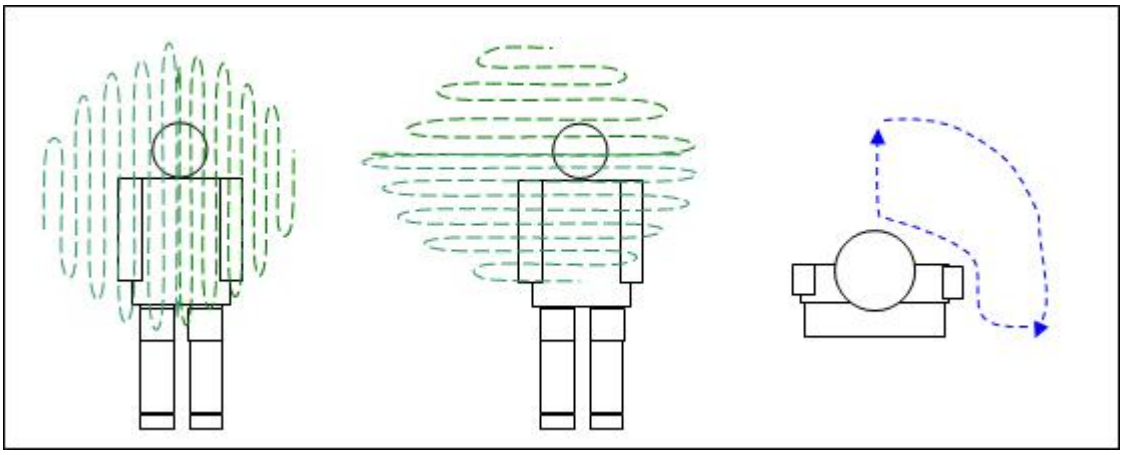

Figure 3. Right hand motions during reach envelope data collection protocol.

Figure 4. Unprocessed 3-D hand position data from Subject 2 during suited

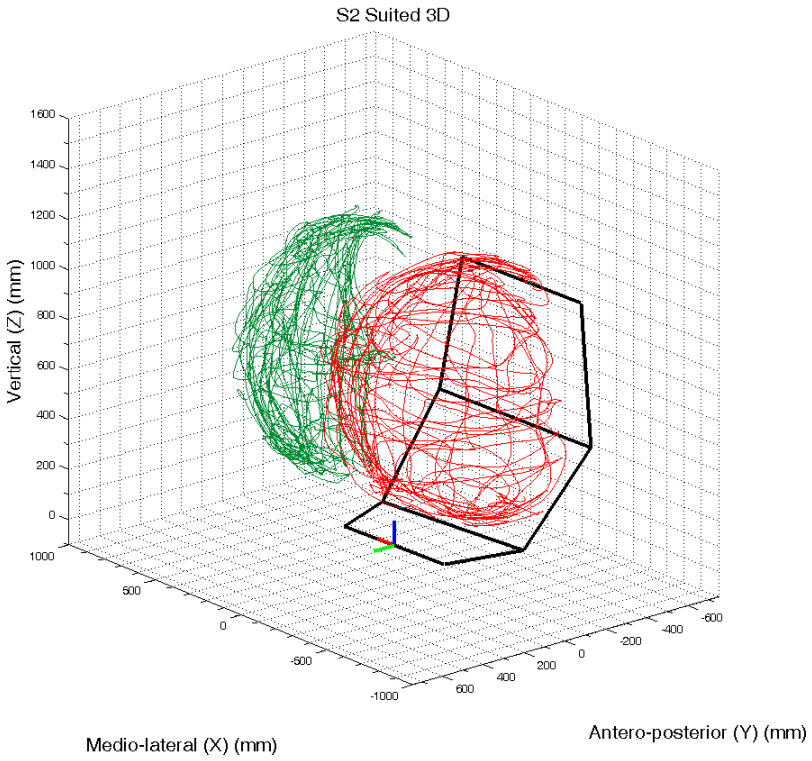

conditions. Red: Left hand, Green: Right hand.

From Figure 4 it can be seen that the unprocessed data provided an incomplete representation of the reach envelopes. Additionally, the 3-D plots did not present the position data in a format that can be easily utilized by the designers of the Mark III suit or the SCOUT vehicle. The analysis routine first utilized the Qhull Delaunay triangulation algorithm (3) to create a mesh from the position data (4), wherein triangles are drawn between sets of data points such that no other data points are contained in any triangle's circumcircle. Each data point was thereby connected to its spatially proximal neighbors and a mesh was then drawn over the surface, providing a more complete representation of the reach envelope (Figure 5).

To enable the triangulated data to be viewed in a format useful for design purposes a computer program was written in which the position data were first displayed from above, from the side, and from behind the chair. The data were then 'sliced' into sections of 10cm thickness. For example, when viewing in the X-Y plane (i.e., from above), the data were presented in multiple plots, each of which displayed X-Y data from a 10cm thick section. The concept is illustrated in Figure 6. Data slices were not presented in the frontal plane because the information was redundant after presentation of data in the other two planes.

In addition to presenting the triangulated areas associated with the position data in each data slice, the unprocessed position data was also included in all plots to provide some indication of the validity of the triangulated data. Position data traced from the left and right hands are shown as red and green lines, respectively.

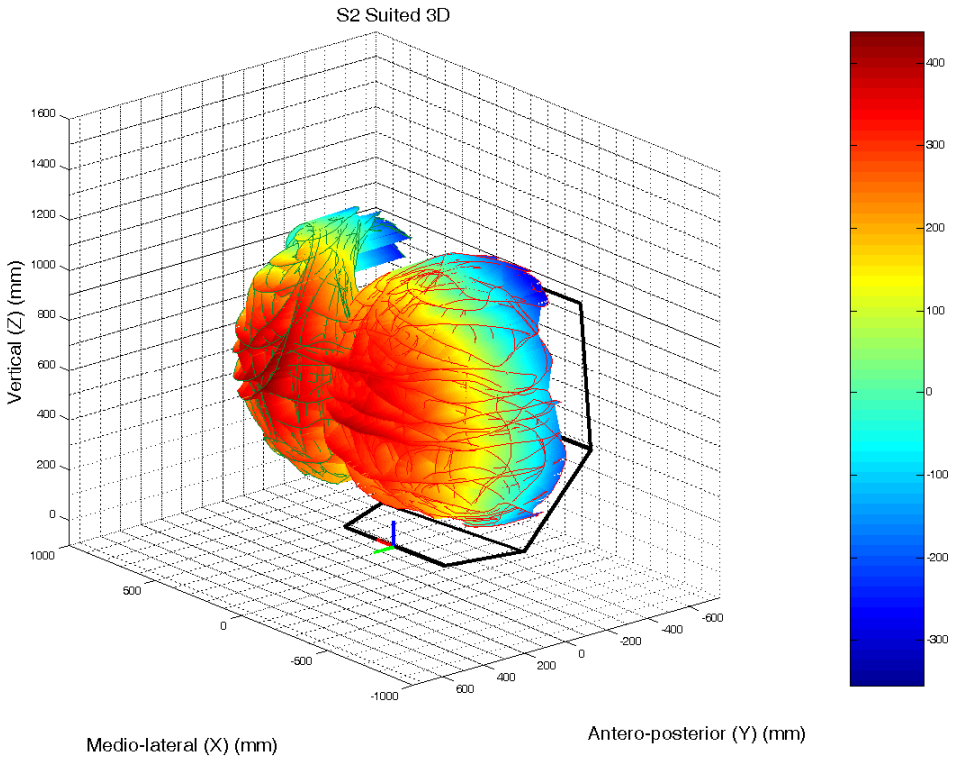

Figure 5. Three-dimensional plot of position data from Subject 2 during suited conditions after applying Delaunay triangulation algorithm.

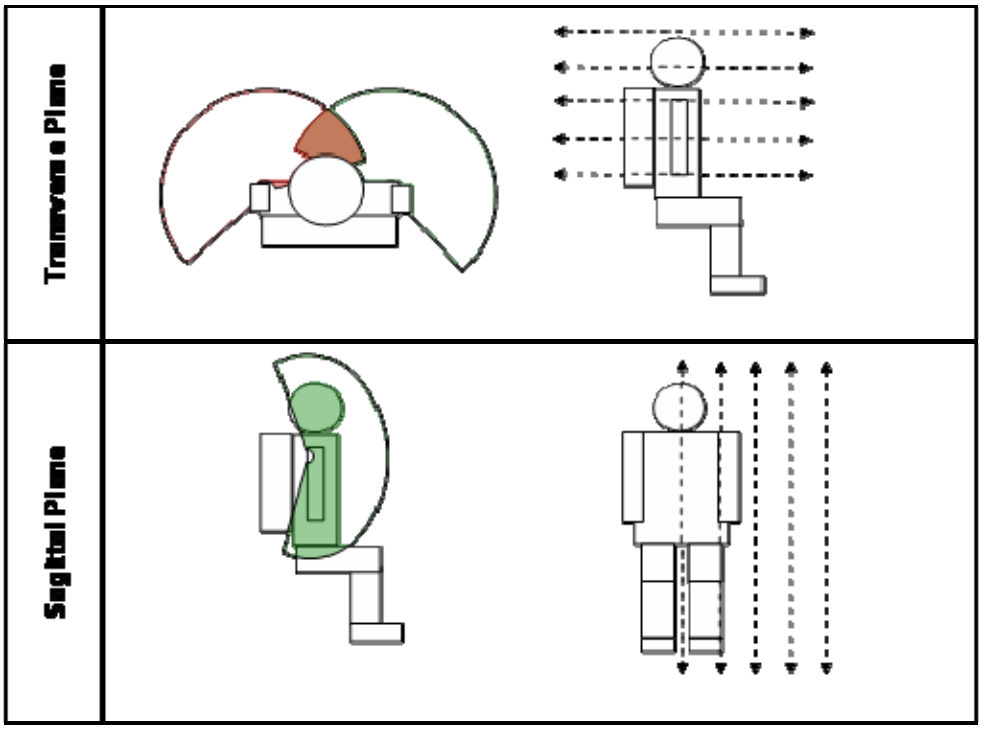

Figure 6. Reach envelope analysis strategy.

Field Testing

Because the motion capture system utilized during laboratory testing is not designed for outdoor use, the evaluation of reach during field testing was performed using Dartfish motion analysis software (Dartfish, Ltd., Fribourg, Switzerland), which is a software program that is used to analyze video footage recorded using standard digital video cameras. Three JVC DVL-9800 video cameras (JVC Company of America, Wayne, NJ) were positioned so as to view the subject from above, from the front, and from the side. An adjustable boom was used to position the overhead camera. The fields of view from each of the three cameras are shown in Figure 7.

Subject 1 was seated in the driver's seat of the SCOUT vehicle while wearing the pressurized Mark III EVA suit. The subject was then instructed to position their left and right hands in a series of low, medium, and high medial and lateral reach positions. Due to the considerable time required to manually extract 3-D hand positions from the 2-D video camera footage using the Dartfish software only 44 hand positions were measured. The inner bounds of the reach envelope were not assessed during field testing.

Using the Dartfish software, the video data were digitized and synchronized. As Figure 7 shows, angular and linear measurements were then taken from the video images using the Dartfish software. To determine the distance represented by each pixel in the image, a line is first drawn along an object in the image of a known length. In this instance, a reference object 59.0 cm in length was positioned within the field of view of each camera and then removed after being used to calibrate the software. As with the laboratory testing, the origin of the coordinate system was positioned at the midpoint of the front edge of the seat pan. Using each camera view, 2-D measurements were then taken to determine the distance of each hand from the origin in the orthogonal axes. Where

possible, measurements were taken in the sagittal and frontal planes (lower two camera views in Figure 7) rather than the overhead view because the overhead camera was not centered exactly above the subject. The 44 hand locations measured during field testing were then compared with the reach envelope determined for Subject 1 during laboratory testing.

The accuracy and reliability of Dartfish is highly dependent upon camera positioning, camera resolution, the distances of the objects from the cameras, the angles of objects and movements with respect to the cameras, and the precision with which the operator can visually identify and mark the positions of the hands in each image. As such, the accuracy of the measurements made using the Dartfish software are unknown for this data collection, but is certainly less than that of the Vicon data recorded in the laboratory setting. The purpose of the field testing was simply to verify that no significant discrepancies existed between the reach and FOV data collected in the laboratory conditions and the data collected under the more realistic field conditions. No significant differences were anticipated.

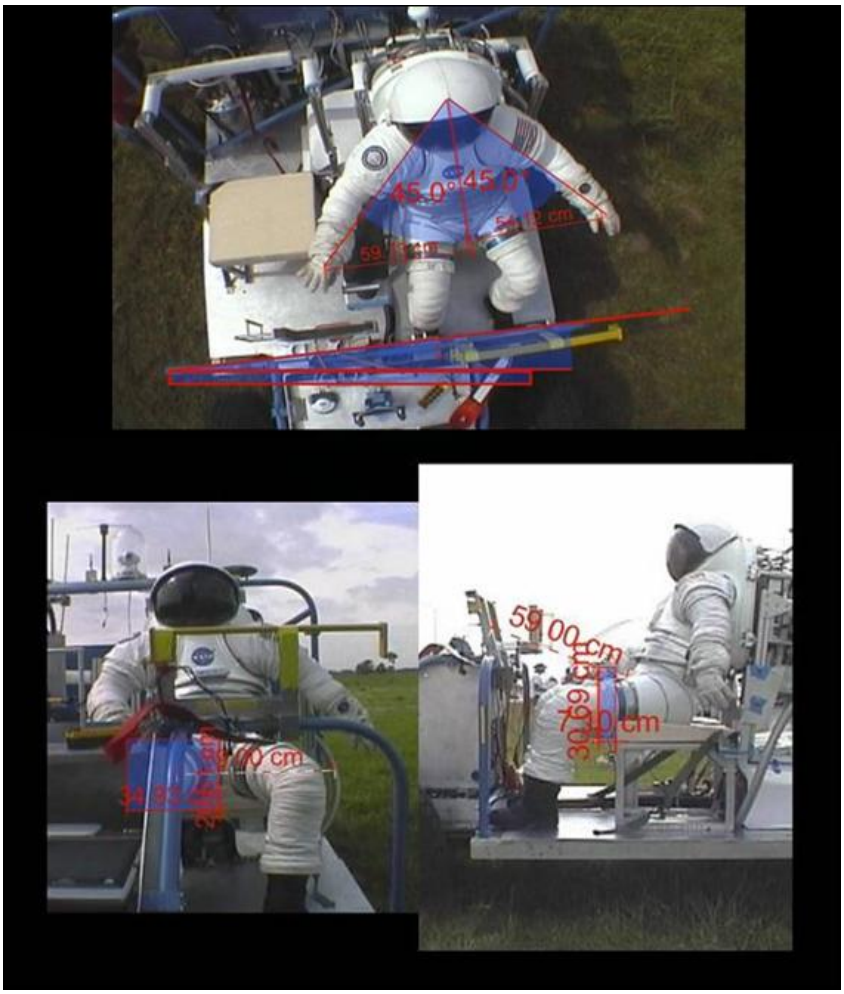

Figure 7. Video camera fields of view.

2.3 FIELD OF VISION MEASUREMENT

Field of Vision (FOV) data were collected during laboratory and field testing sessions. During laboratory testing, FOV was tested during shirtsleeve and suited conditions. FOV was tested only during suited conditions during field testing.

A socket with an attached plumb line was slowly moved forward at eye level from behind the subject's head until the subject indicated that the socket became visible. At this instance, the point on the ground directly beneath the plumb line was marked (Figure 8, left). The position of the eyes was marked on the ground in order to provide a reference for measuring angles, as shown in Figure 9. The 2-D positions of the eyes and the target in the transverse plane during laboratory testing were manually measured from the marks on the floor using a tape measure and were measured using Dartfish analysis of video data during field testing.

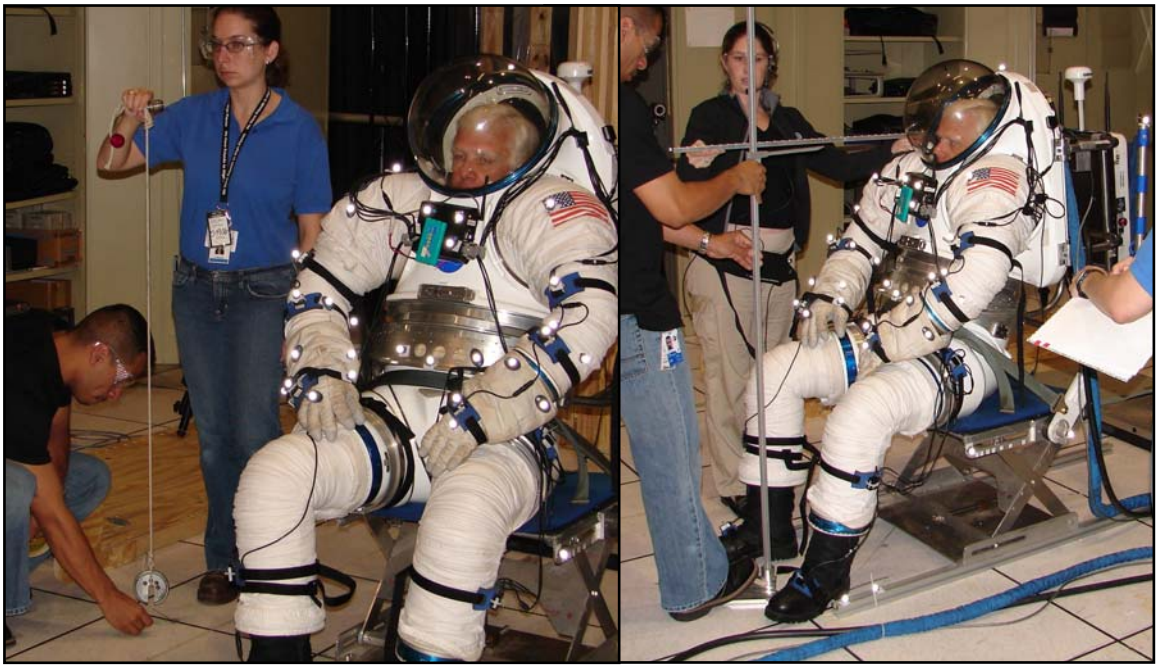

Figure 8. Lateral (left image) and Vertical (right image) Field of Vision testing protocol.

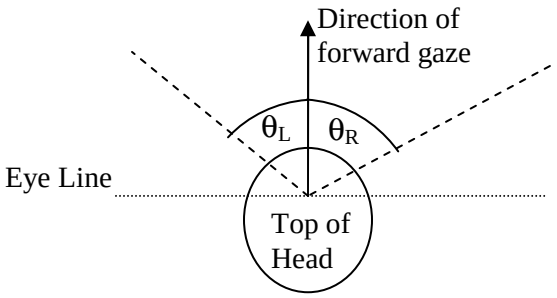

Figure 9. A line was marked on the ground to designate the location of the subject's eyes, which was used as an origin to measure visual angles.

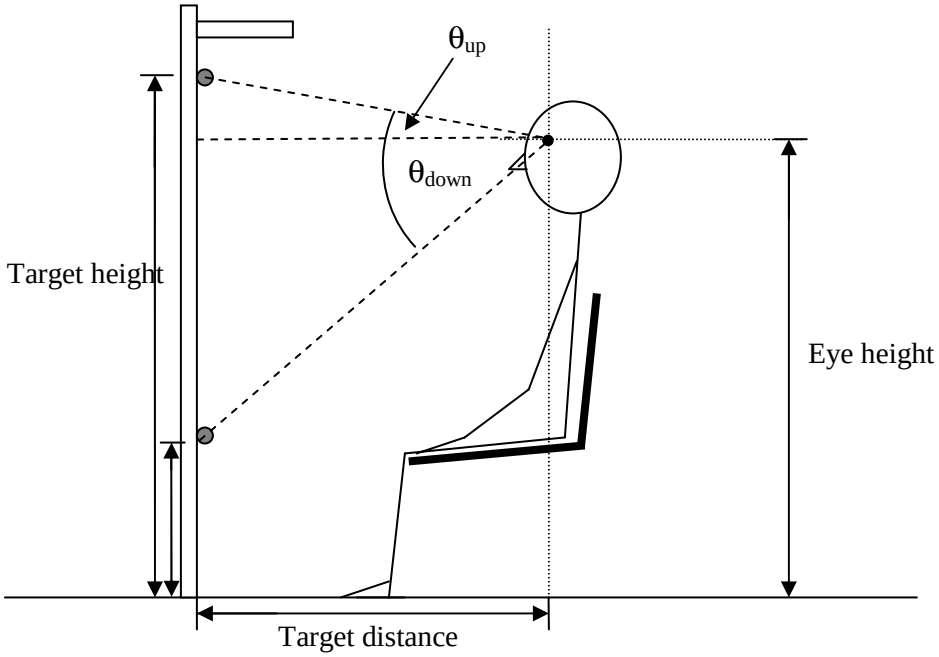

Figure 10. Sagittal plane Field of Vision measurement method.

The procedure was also performed while moving the socket slowly upward and downward directly in front of the subject (Figure 8, right). The socket was brought from a mid-level height slowly up the length of an anthropometer until the subject indicated that it had risen above the field of vision. The vertical distance between the target and the ground was recorded. Beginning again from a mid-level height, the socket was brought slowly down the length of the anthropometer until the subject indicated that it was below his field of vision. The procedure was performed three times for each condition. The maximum field of vision for each condition was used in the subsequent analysis. The field of vision angles in the sagittal plane were then calculated from the 2-D positions of the eyes and socket as measured by the anthropometer, measuring tape, and Dartfish analysis (during field testing) as illustrated in Figure 10.

For the FOV measurements in the transverse plane (left-right FOV), the process was performed under two conditions. Under the first condition 'fixed' subjects were instructed to keep their head facing forwards while in the second condition 'turning' subjects were instructed to move their head so as to maximize their FOV. In the sagittal plane (vertical FOV) only 'fixed' condition measures were made.

3. RESULTS

The reach envelopes calculated during laboratory testing for Subjects 1 and 2 are shown in the following pages. The 44 reach envelope hand positions determined from Subject 1 using Dartfish analysis of field testing data are shown as black points. For purposes of comparison, data for suited and shirtsleeve conditions are shown side-by-side.

For each Subject, the first images display the 3-D hand position data after applying the Delaunay triangulation algorithm. Subsequent figures then show the same data as viewed from the side, from above, and from behind. The coloring of each figure corresponds to the position in one of the three axes and is explained in the associated captions. The 10 cm slices (or planes) into which each reach envelope was divided are super-imposed on the figures of the side and rear views. The reach envelope within each of those planes is then shown in the subsequent figures. Cross-sections of reach envelopes that did not differ greatly from each other are grouped together and combined into single figures. The title of each figure indicates the specific plane(s) represented in that figure. A comparison of suited reach envelopes between subjects is shown in Figure 25.

Also shown on the side and front views (Figures 15-18) are the FOV data. The blue and red lines represent FOV angles under the ‘fixed’ and ‘turning’ conditions, respectively. In Figure 26, the FOV data from left and right sides are averaged and shown in bar graphs for comparison between conditions.

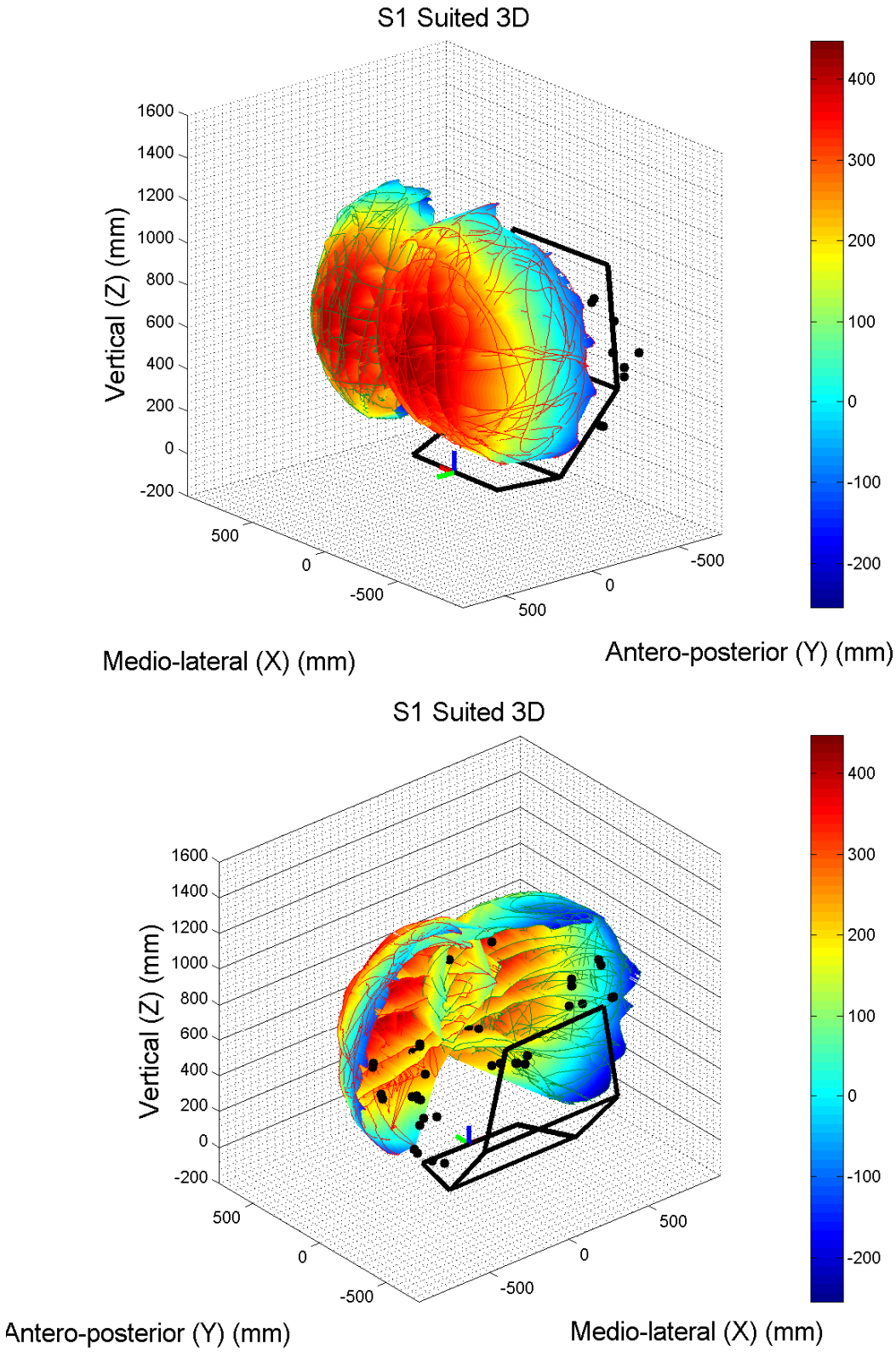

Figure 11. Three-dimensional view of triangulated reach envelope for Subject 1 suited. Colorbar = Y position (mm).

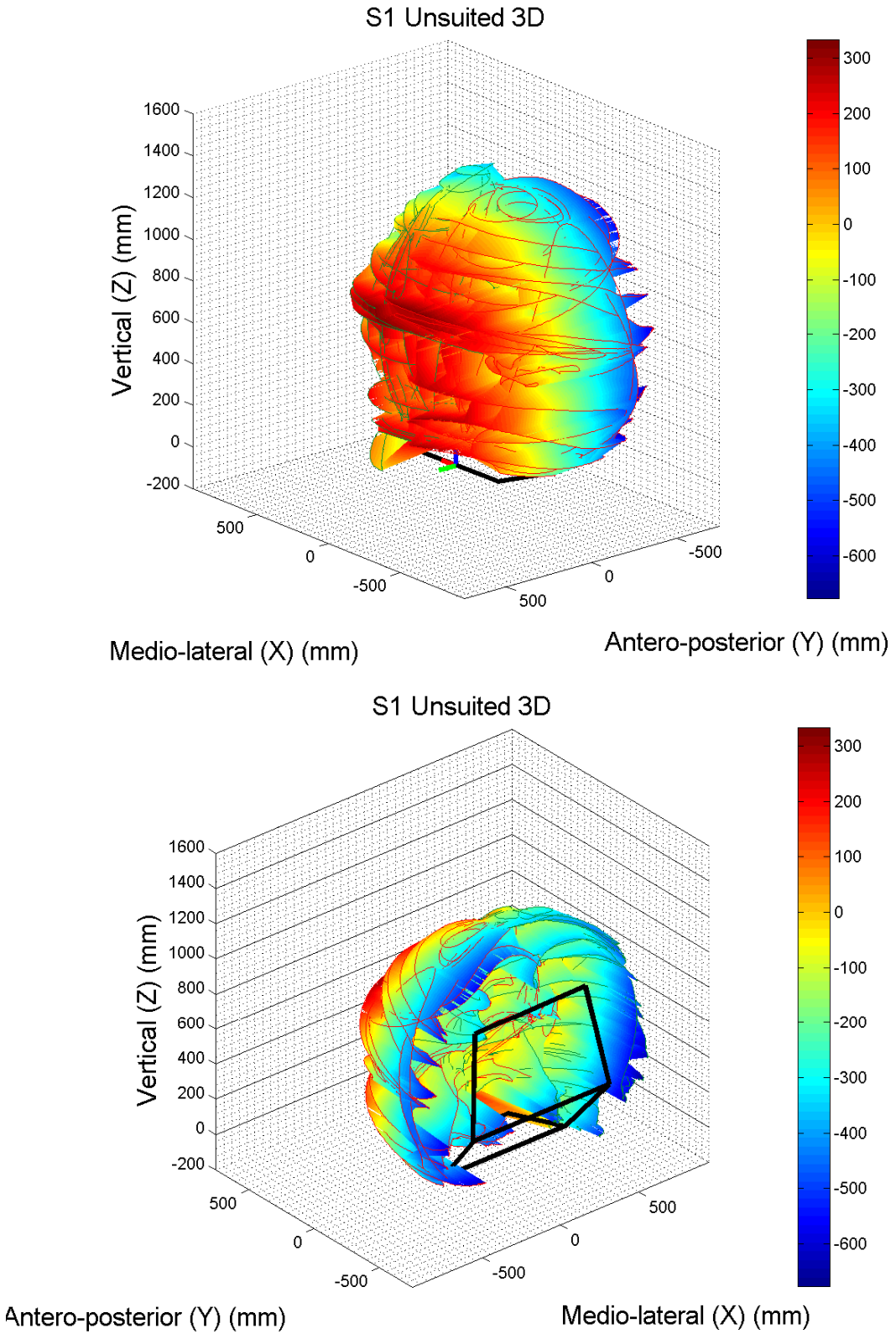

Figure 12. Three-dimensional view of triangulated reach envelope for Subject 1 unsuited. Colorbar = Y position (mm).

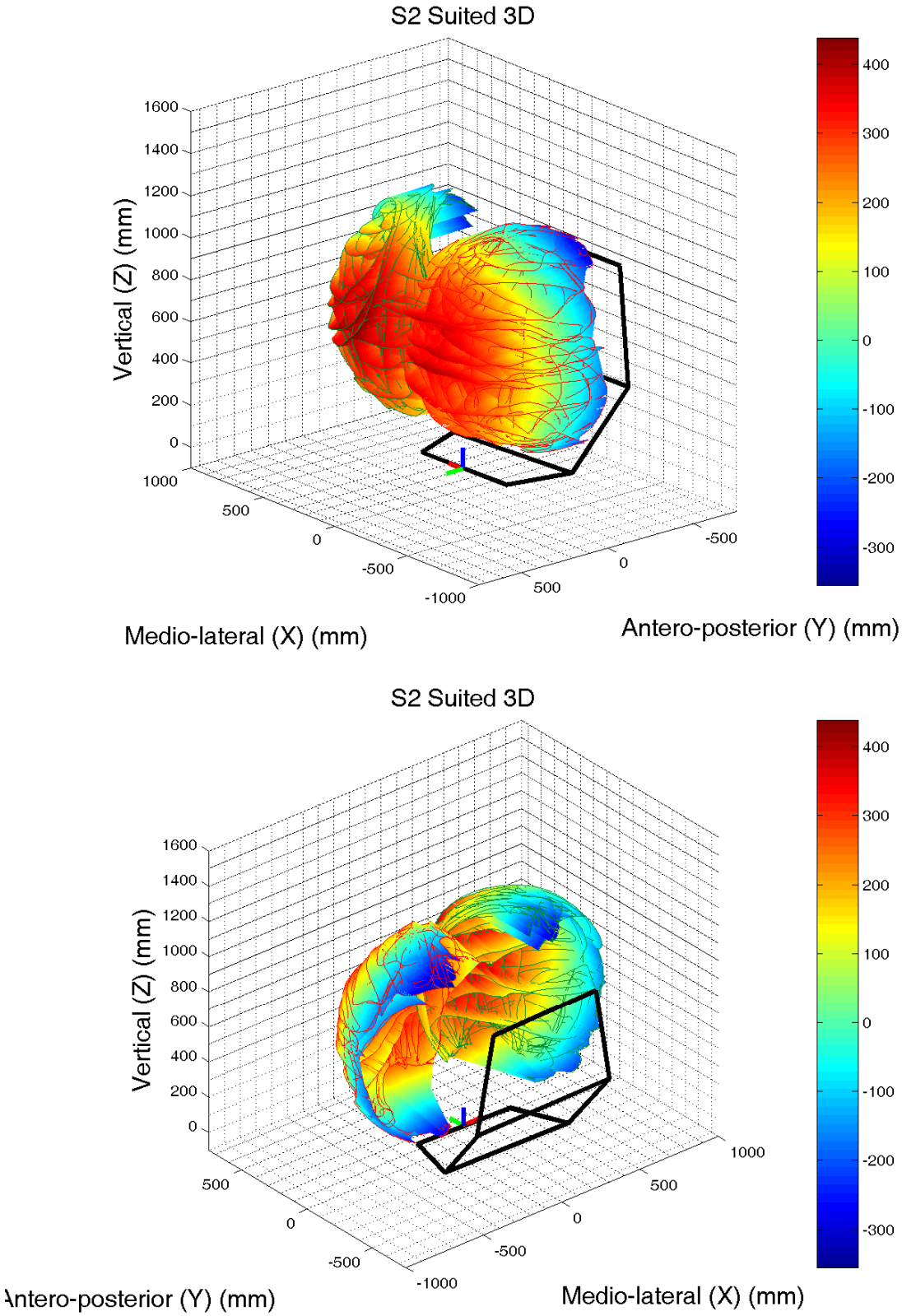

Figure 13. Three-dimensional view of triangulated reach envelope for Subject 2 suited. Colorbar = X position (mm).

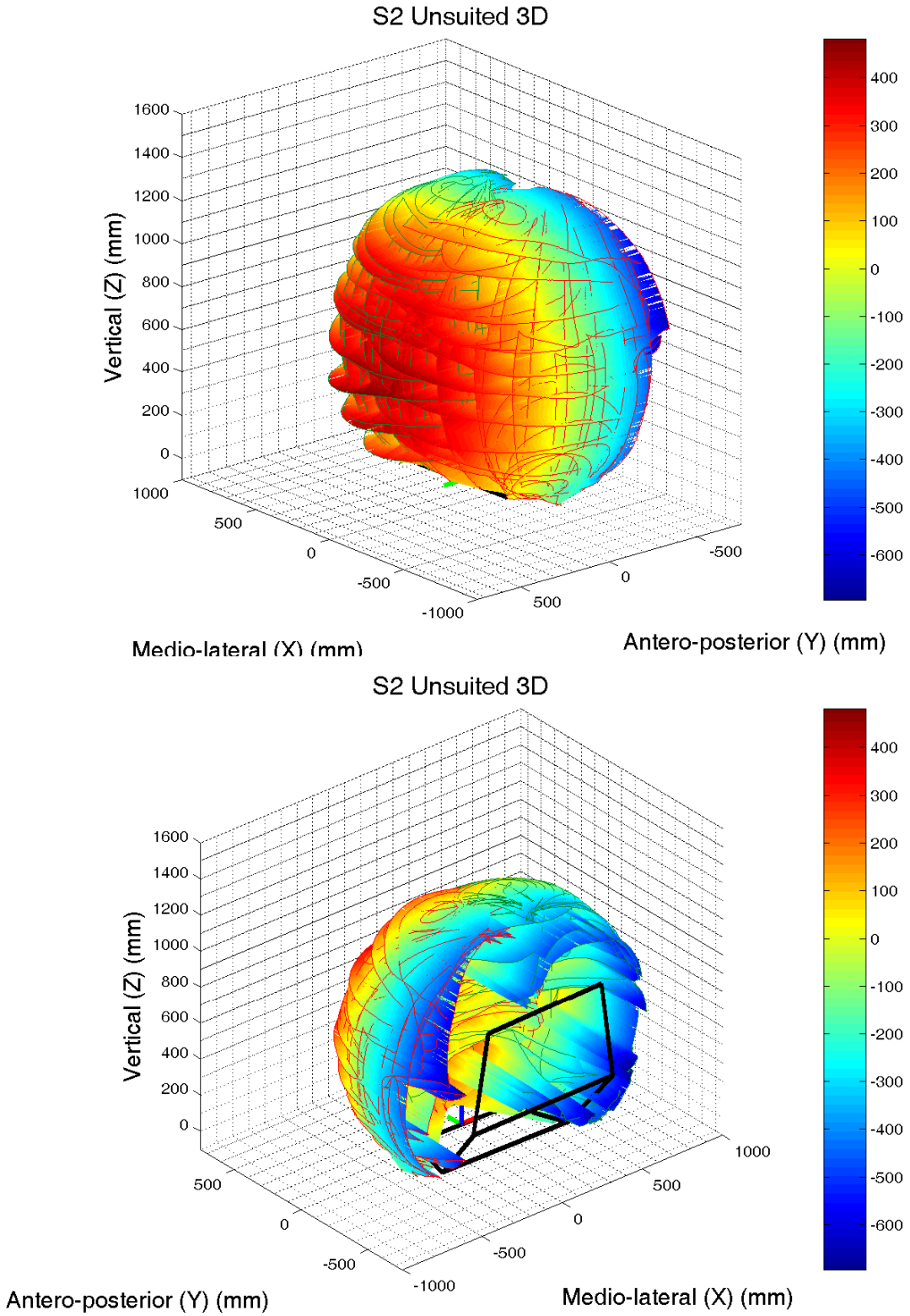

Figure 14. Three-dimensional view of triangulated reach envelope for Subject 2 unsuited. Colorbar = Y position (mm).

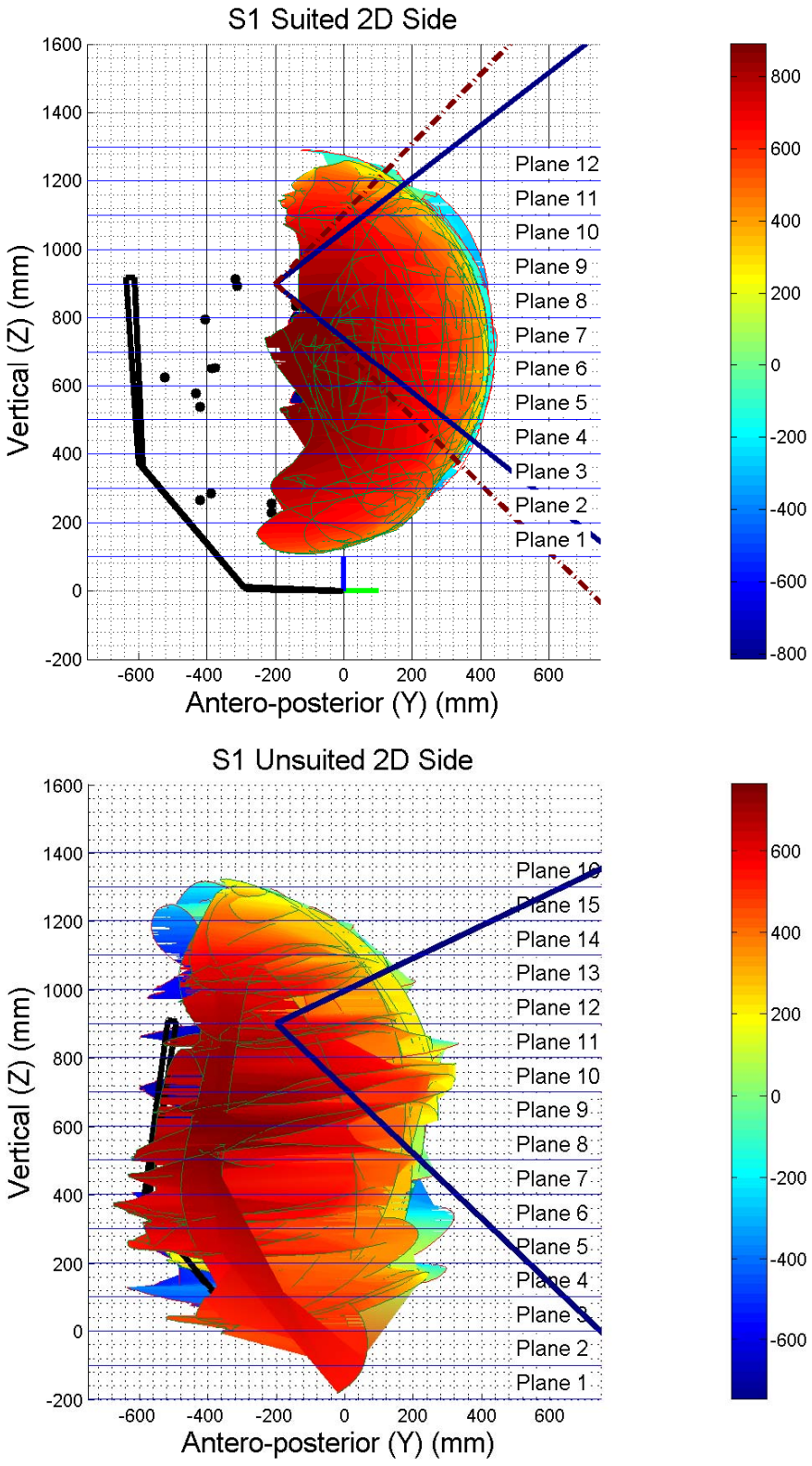

Figure 15. Triangulated reach envelope and field of vision data for Subject 1 suited and unsuited viewed from side (Field = dot-dash line). Colorbar = X position (mm).

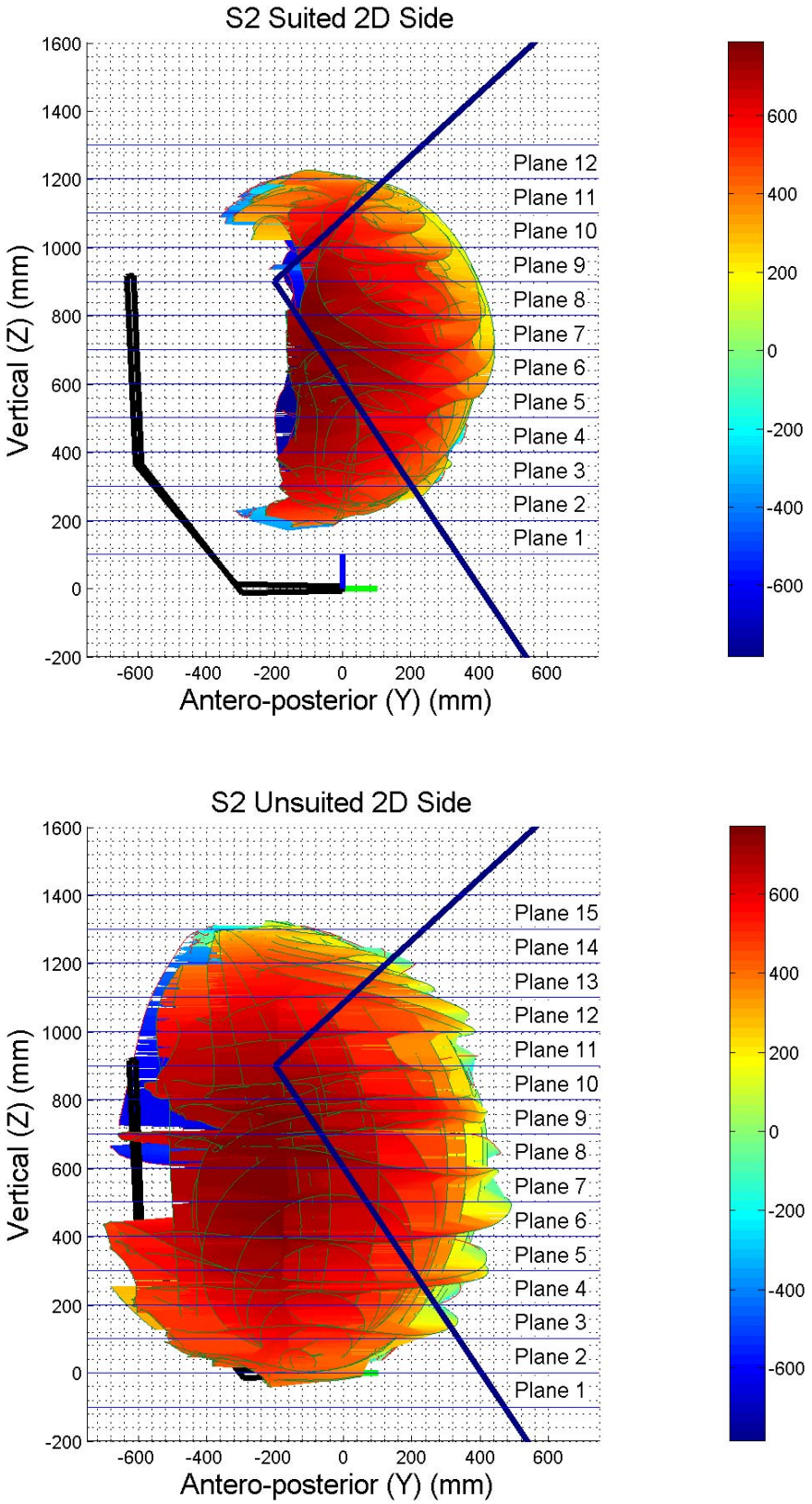

Figure 16. Triangulated reach envelope and field of vision data for Subject 2 suited and unsuited viewed from side. Colorbar = X position (mm).

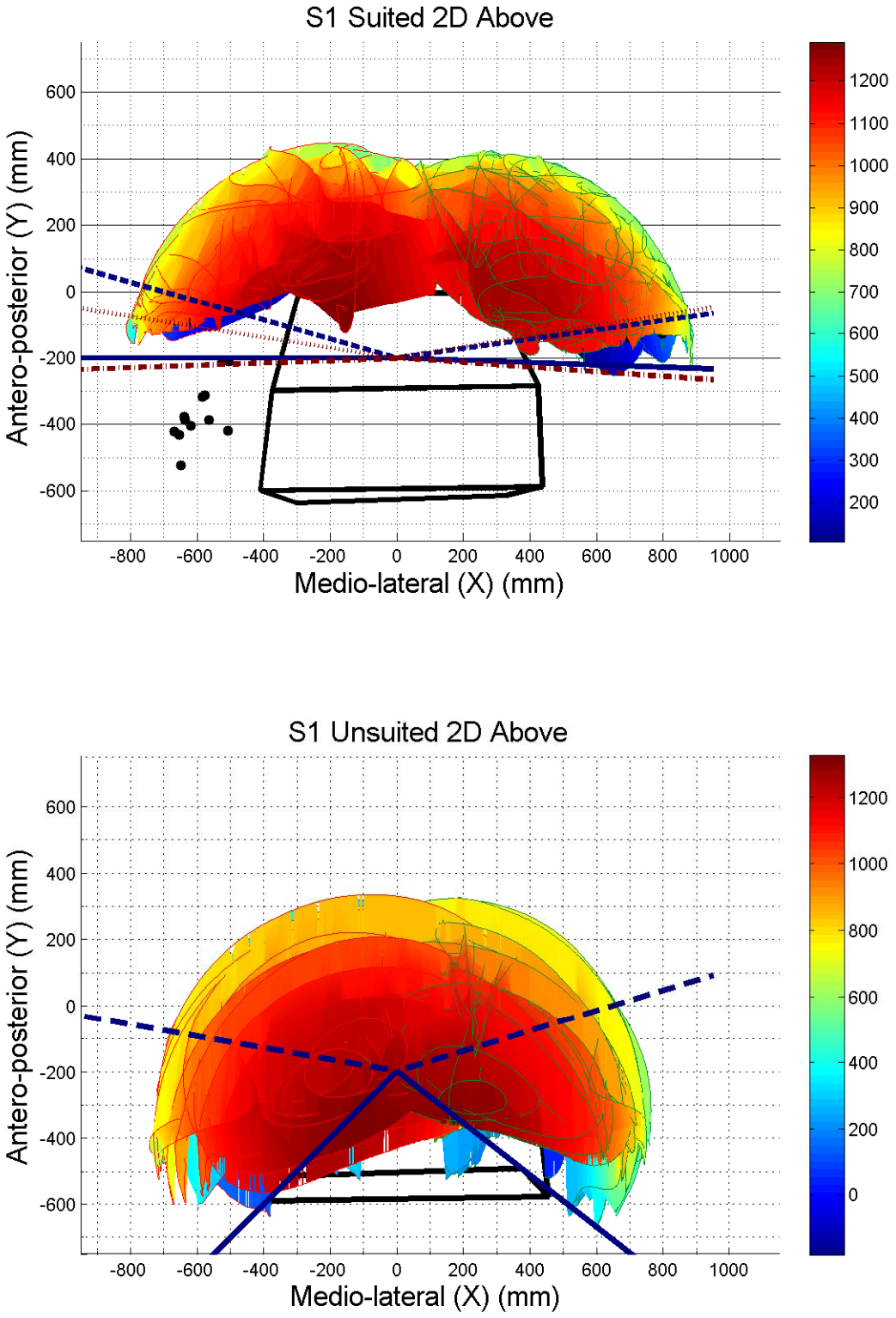

Figure 17. Triangulated reach envelope and field of vision data for Subject 1 suited and unsuited viewed from above (Laboratory Fixed = blue dash line; Field Fixed = red dot line; Laboratory Turning = solid blue line ; Field Turning = red dash-dot line). Colorbar = Z position (mm).

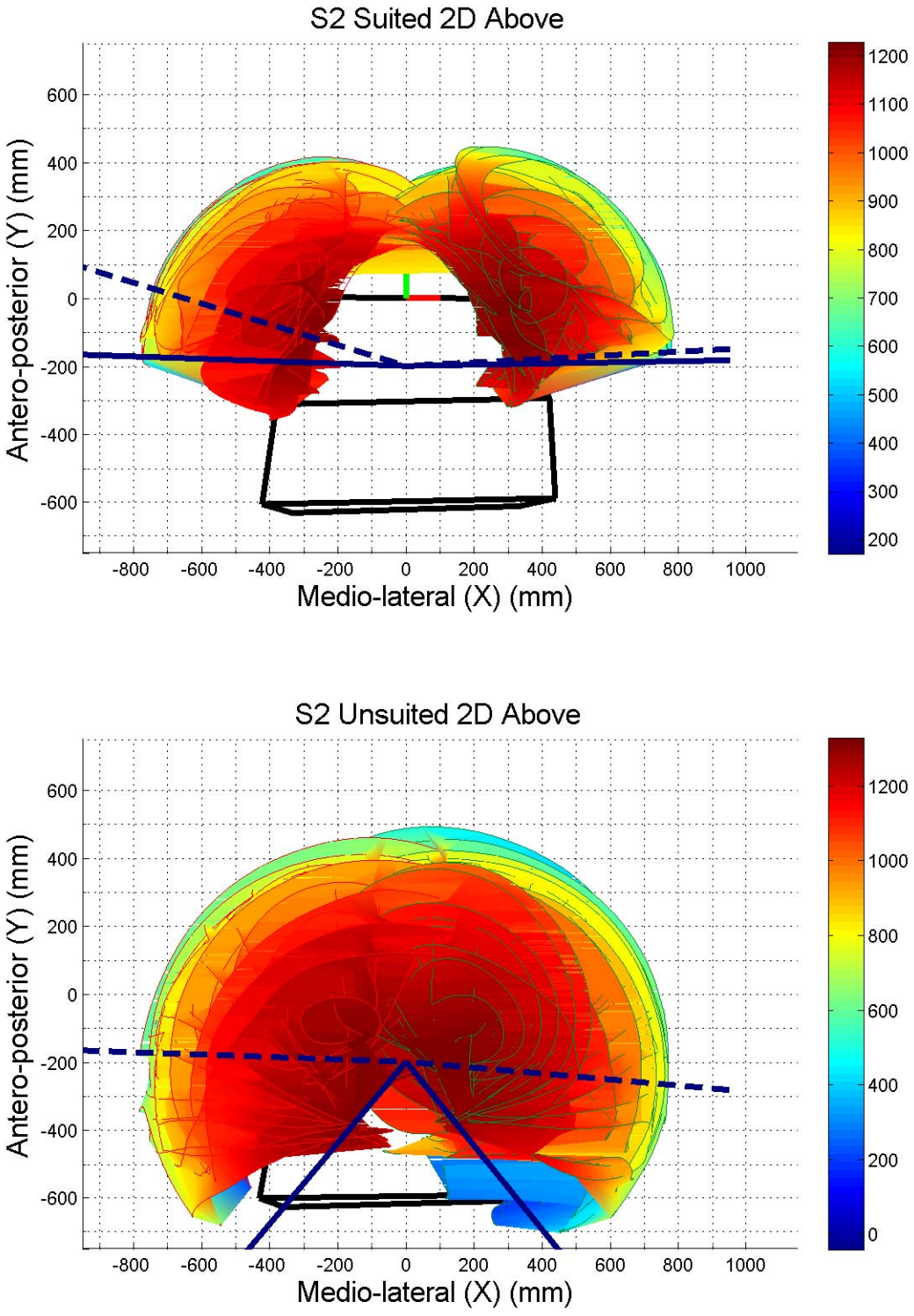

Figure 18. Triangulated reach envelope and field of vision data for Subject 2 suited and unsuited viewed from above (Laboratory Fixed = blue dash line; Laboratory Turning = solid blue line). Colorbar = Z position (mm).

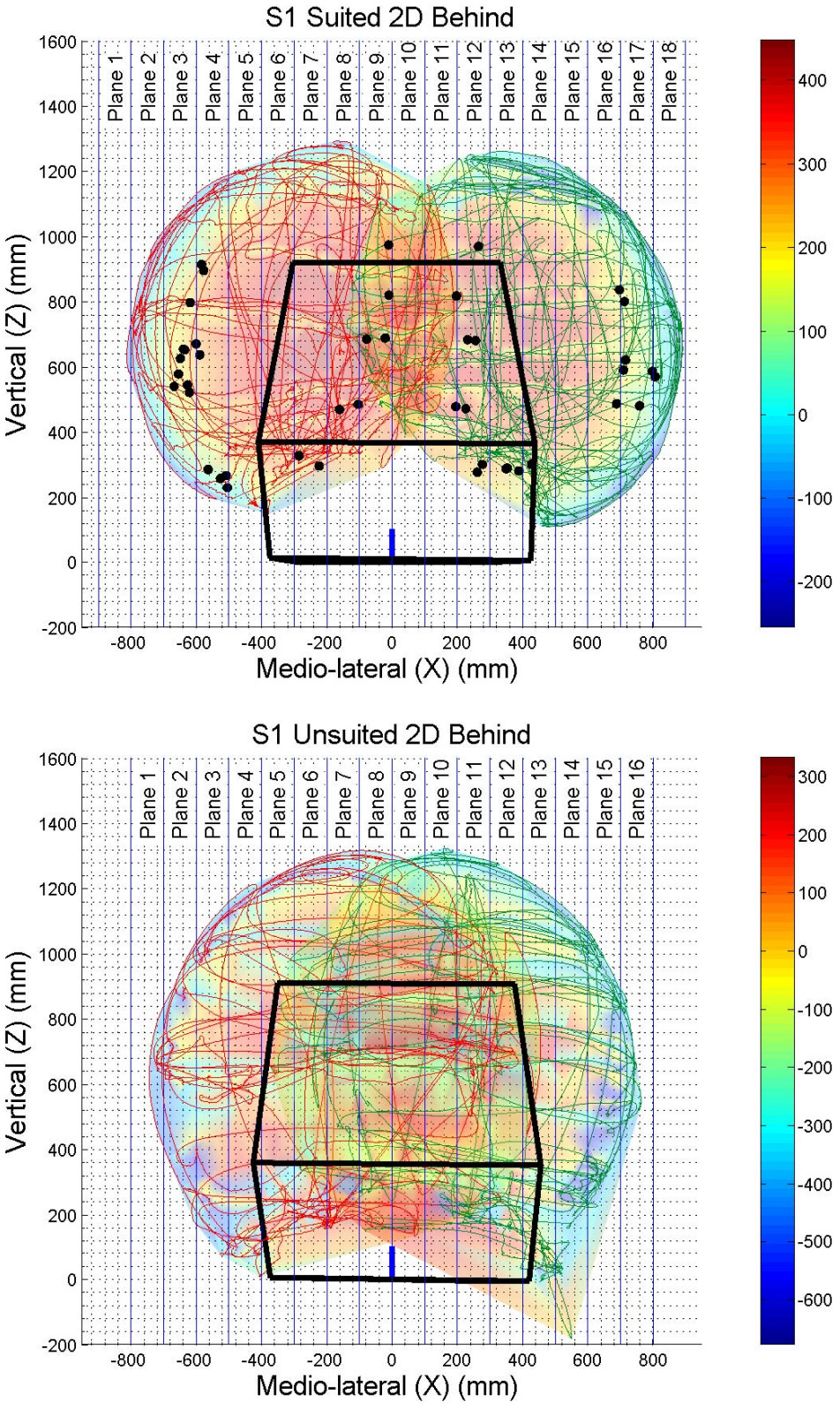

Figure 19. Triangulated reach envelope and field of vision data for Subject 1 suited and unsuited viewed from behind. Colorbar = Y position (mm).

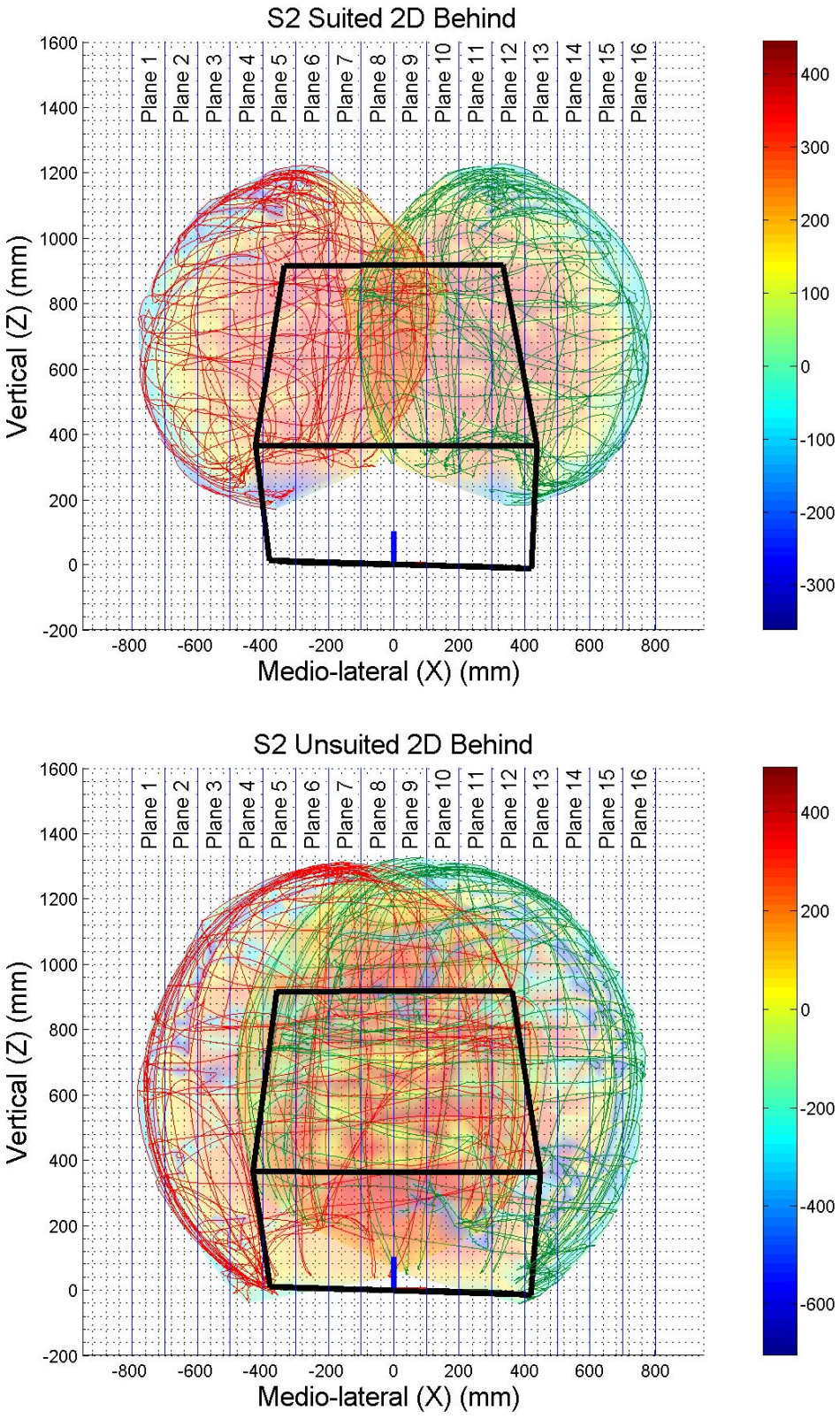

Figure 20. Triangulated reach envelope and field of vision data for Subject 2 suited and unsuited viewed from behind. Colorbar = Y position (mm).

Suited	Unsuited
[No suited reach envelope within these planes]	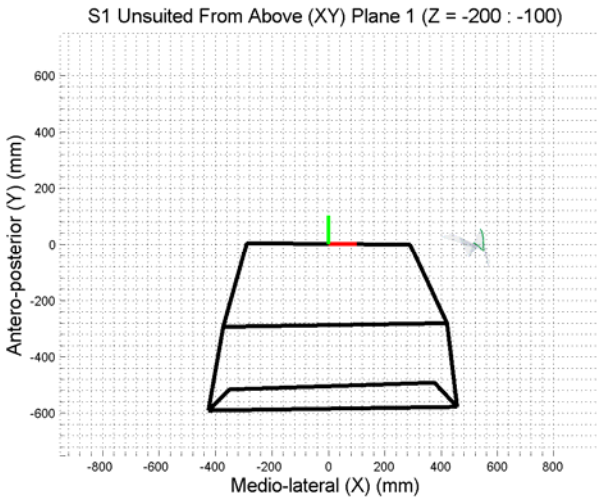 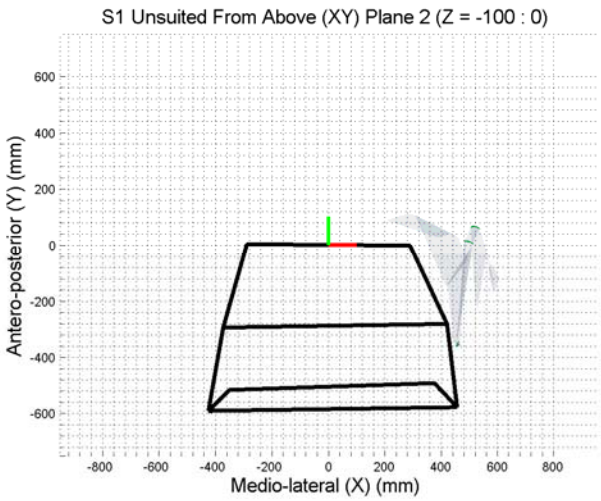 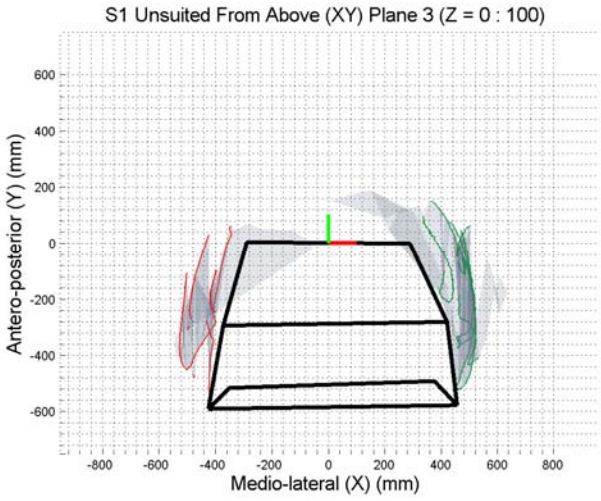

Suited Unsuited

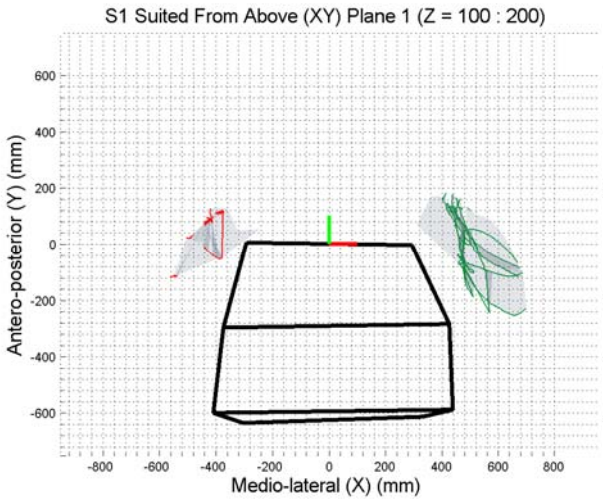

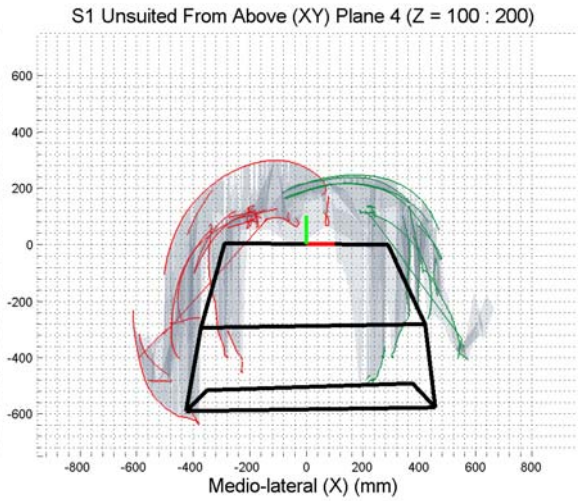

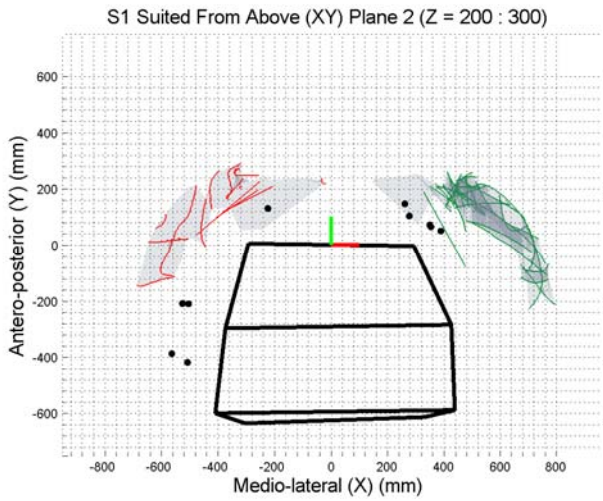

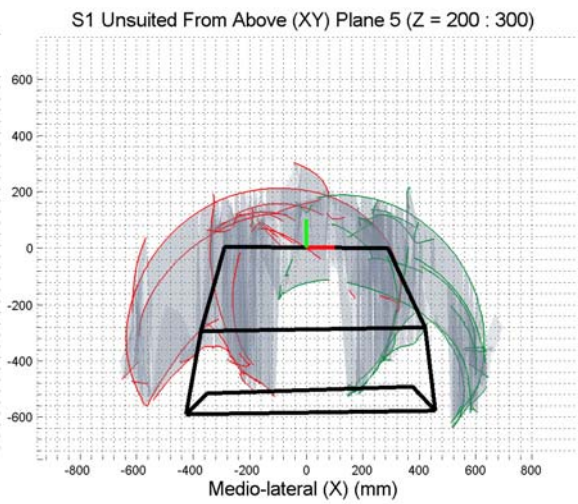

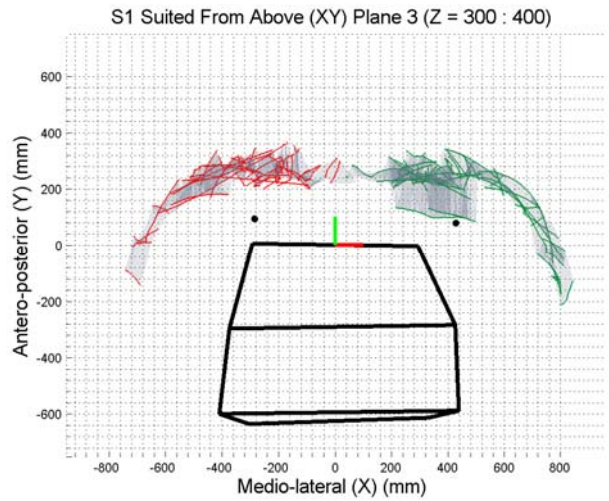

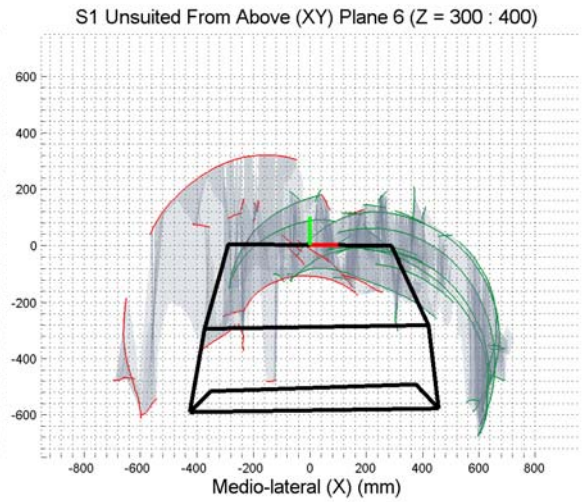

Suited

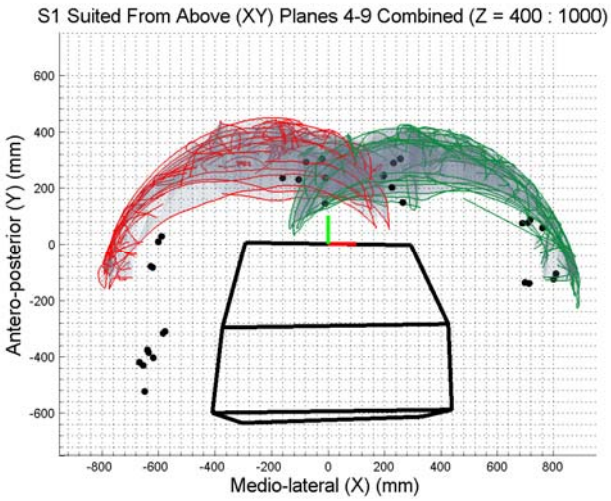

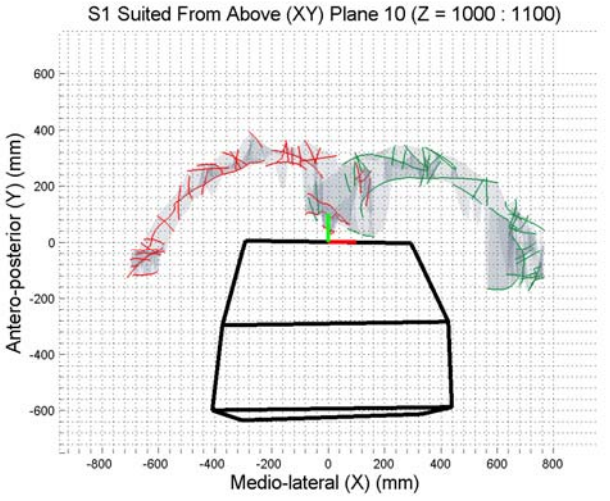

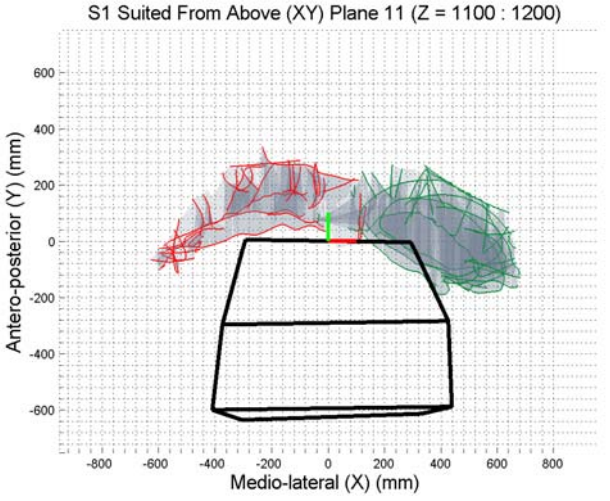

Unsuited

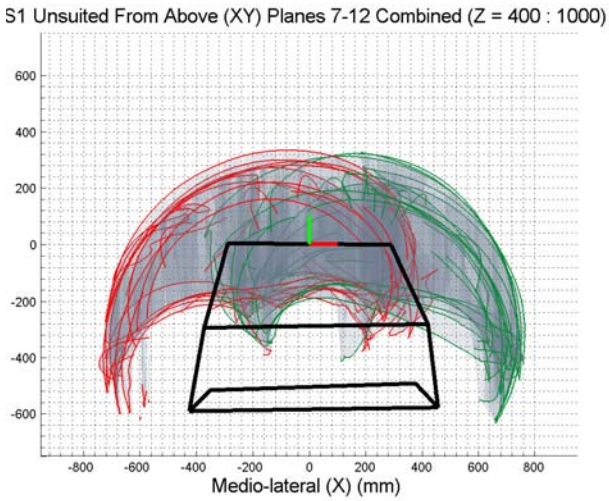

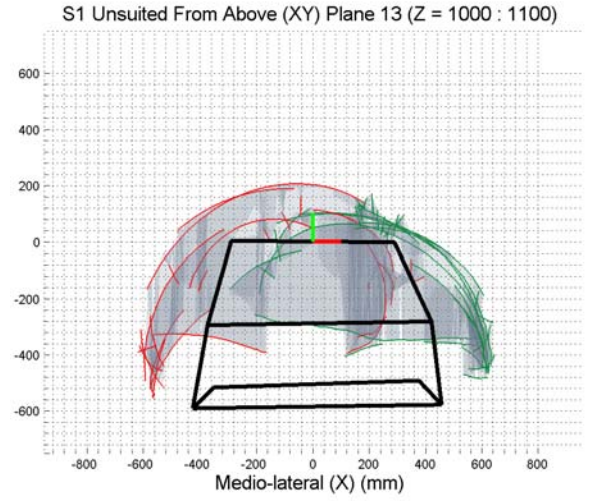

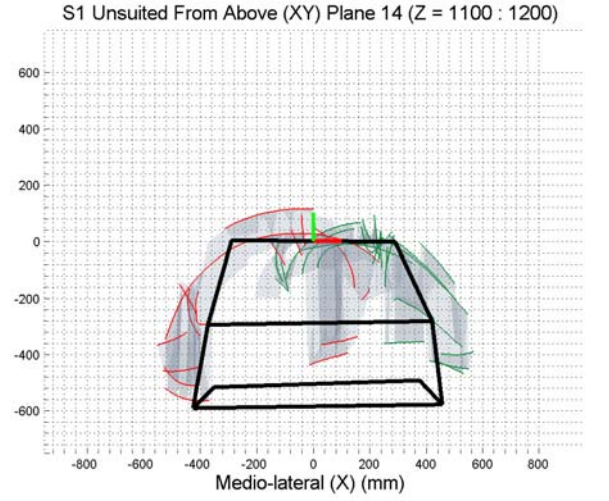

Suited Unsuited

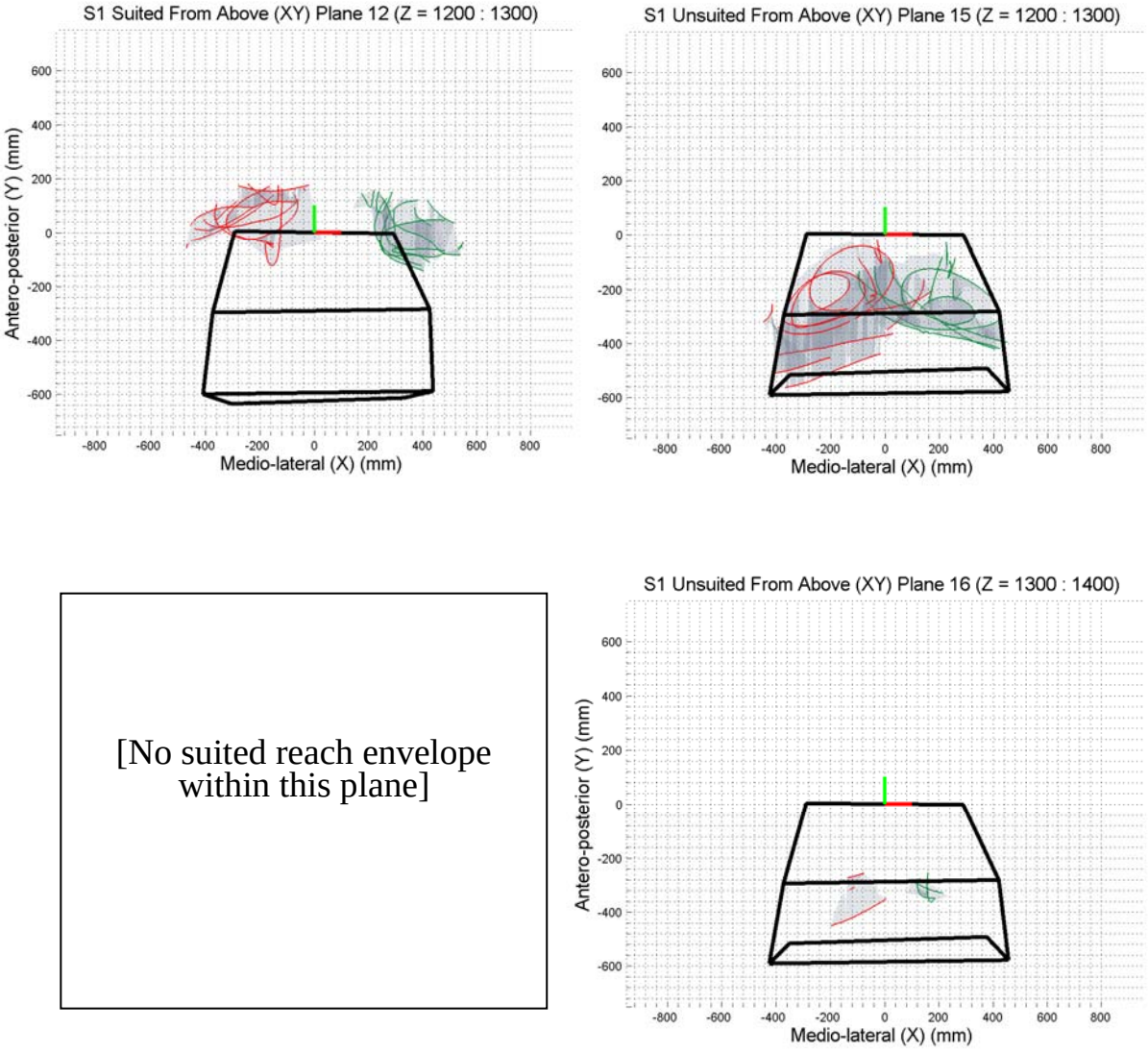

Figure 21. Triangulated reach envelope transverse plane cross-sectional slice data for Subject 1 suited and unsuited.

Suited	Unsuited
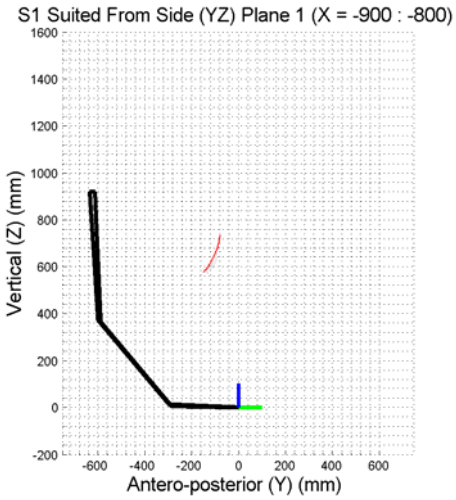	[No unsuited reach envelope within this plane]
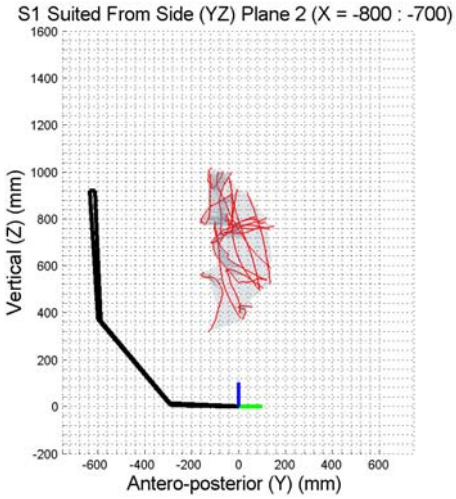	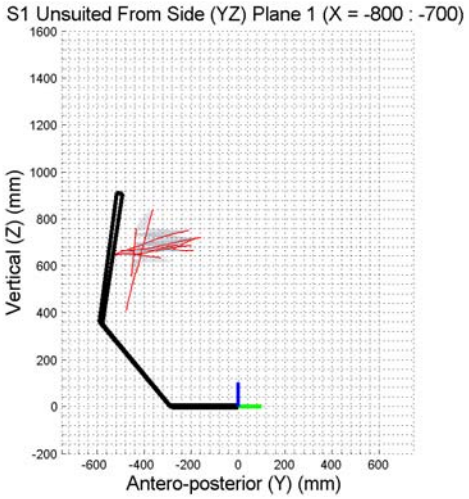
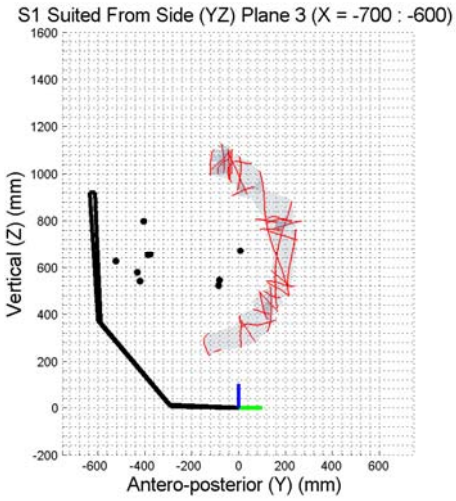	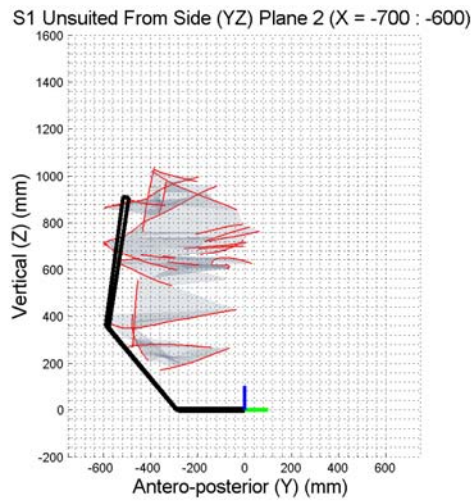

Suited

Unsuited

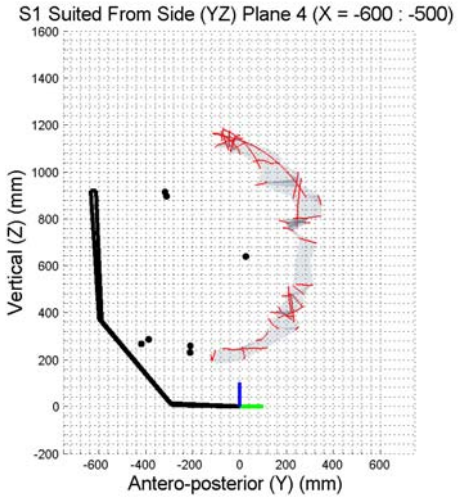

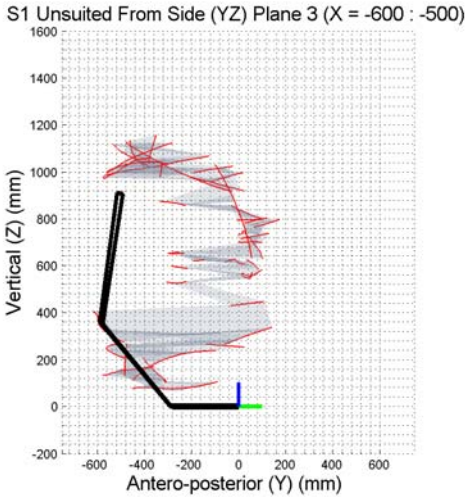

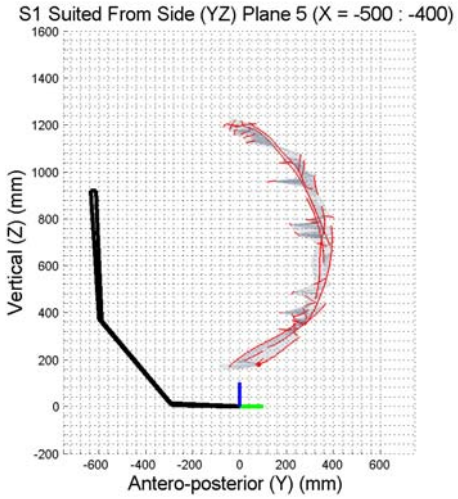

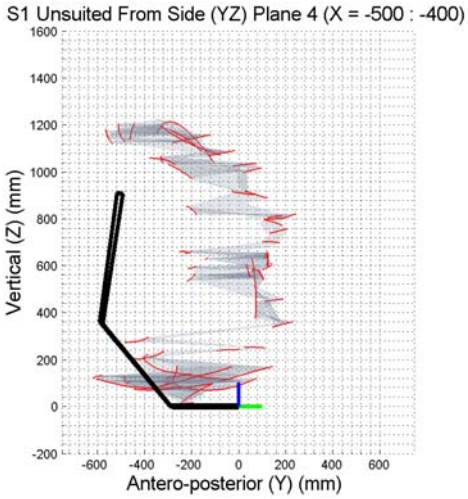

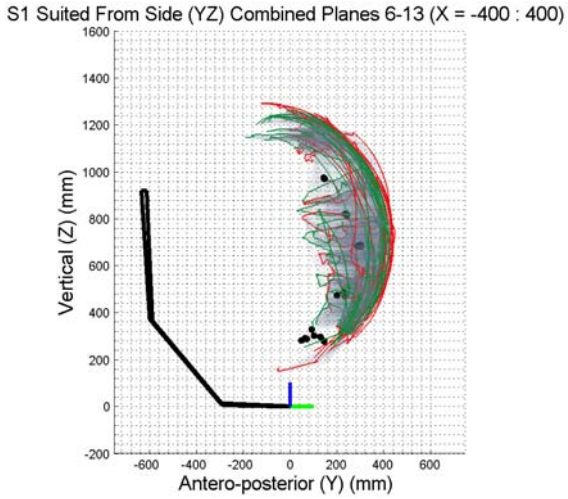

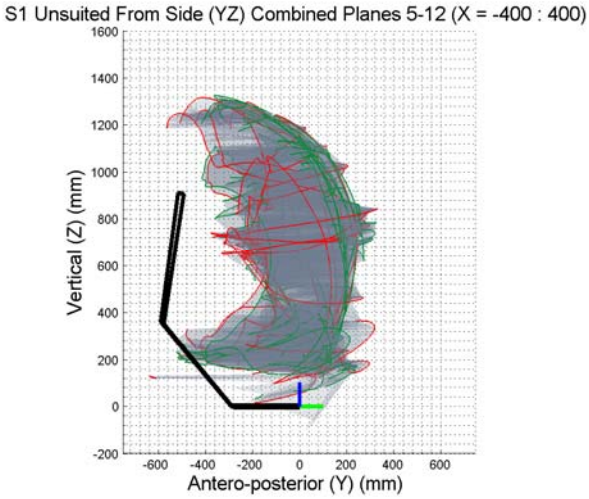

Suited

Unsuited

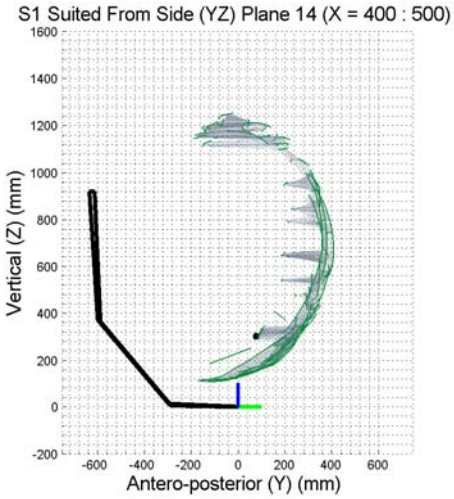

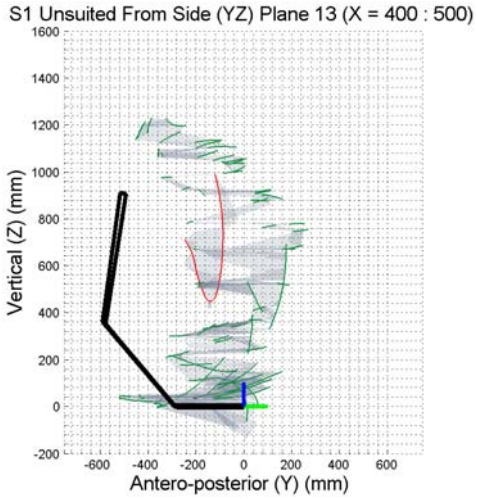

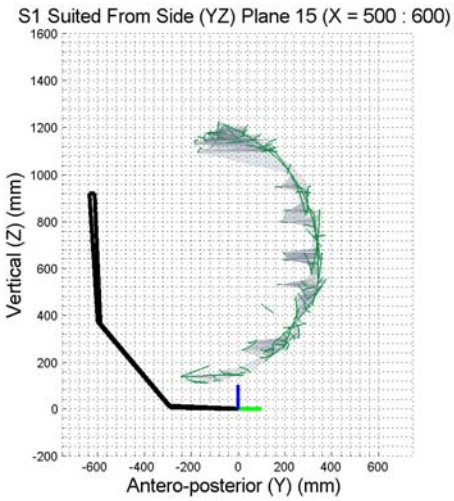

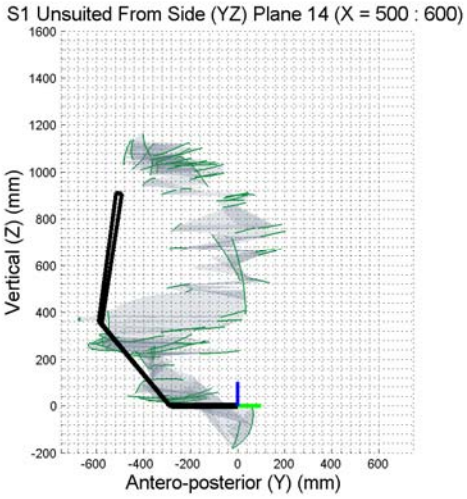

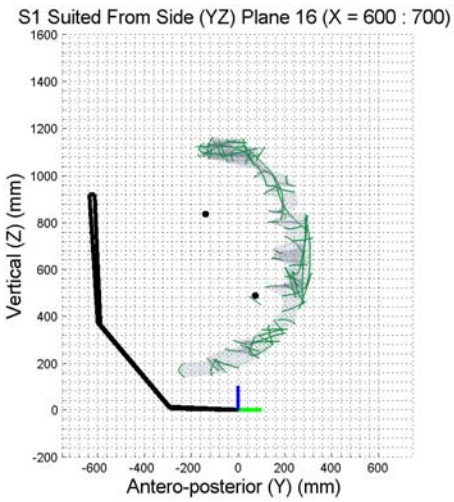

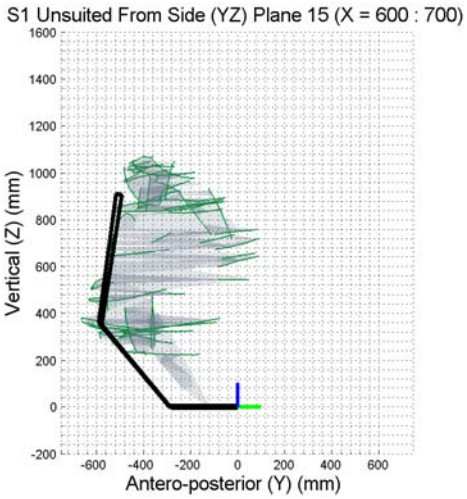

Suited

Unsuited

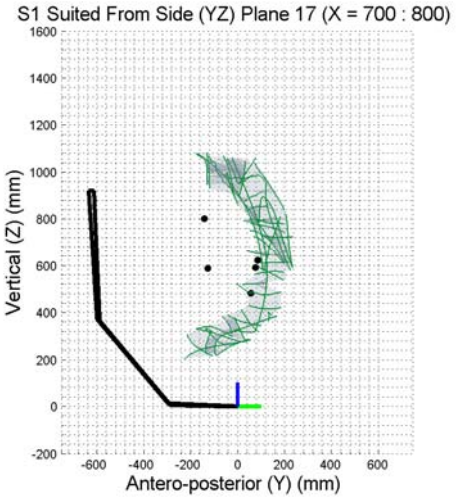

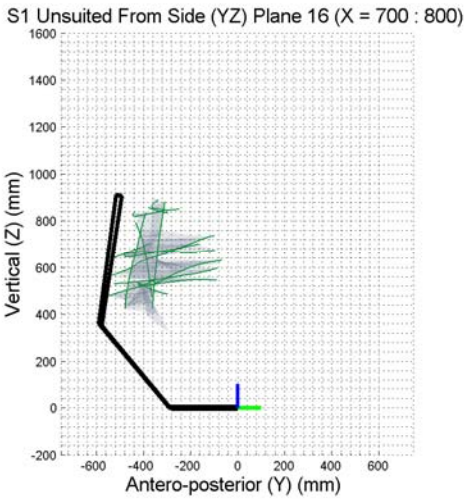

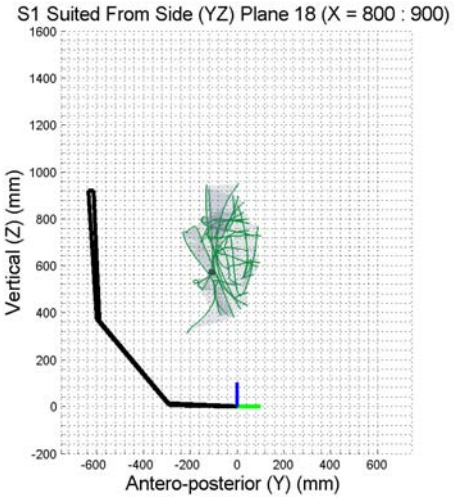

[No unsuited reach envelope within this plane]

Figure 22. Triangulated reach envelope sagittal plane cross-sectional slice data for Subject 1 suited and unsuited.

Suited	Unsuited
[No suited reach envelope within this plane]	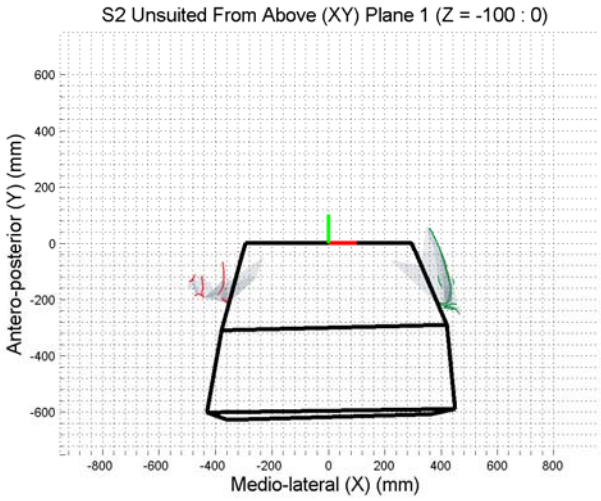
	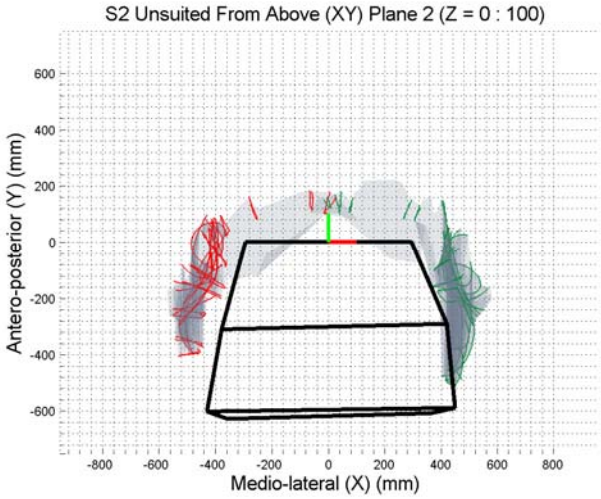
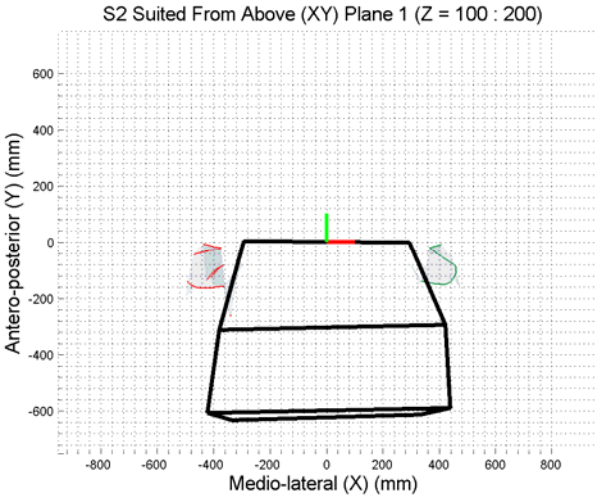	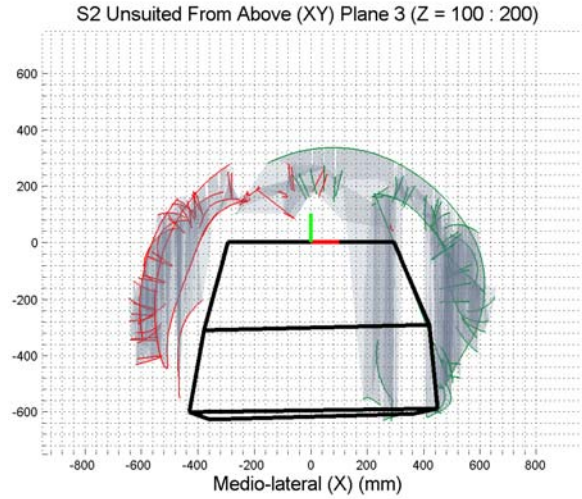

Suited Unsuited

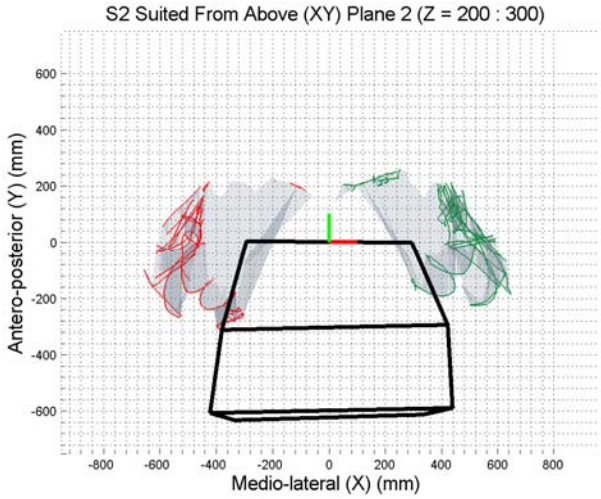

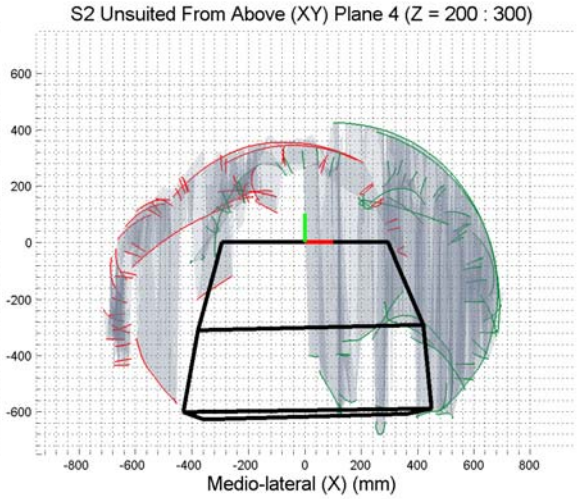

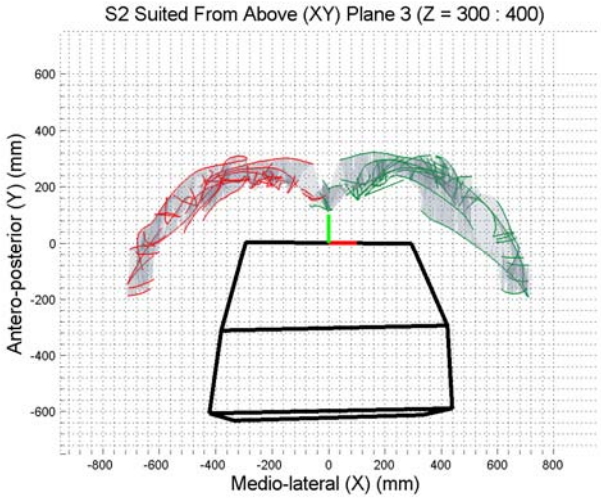

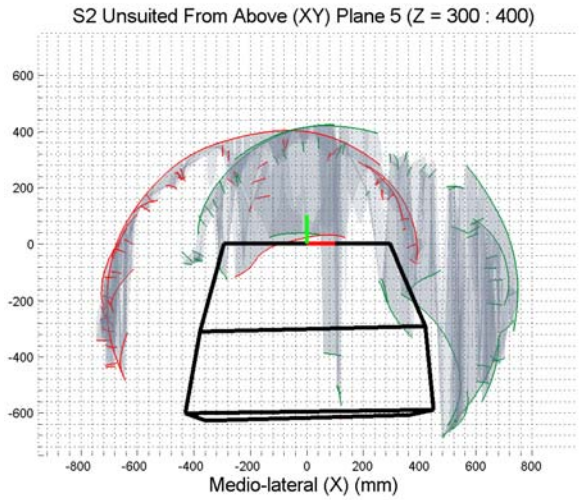

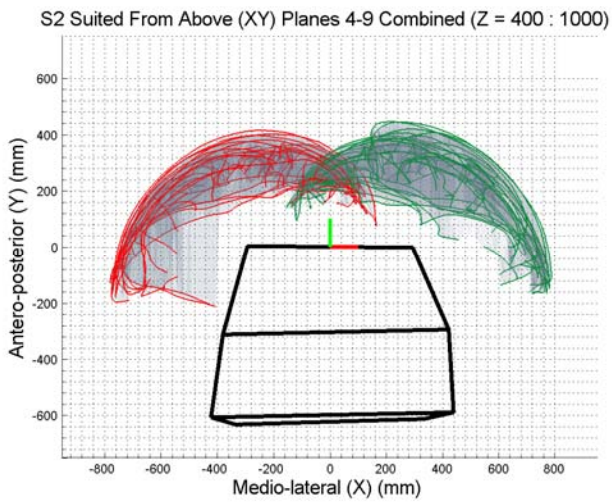

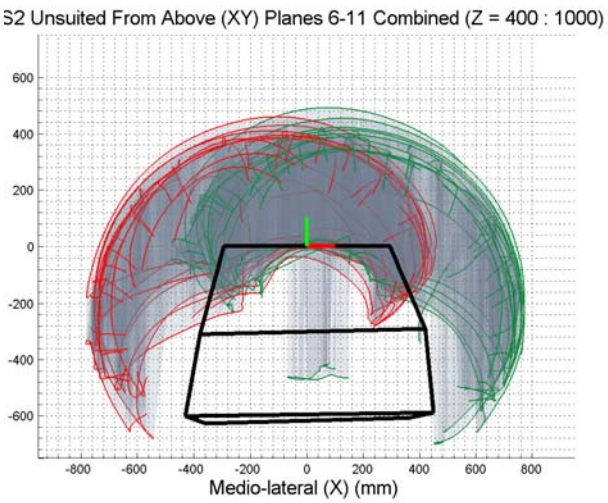

Suited

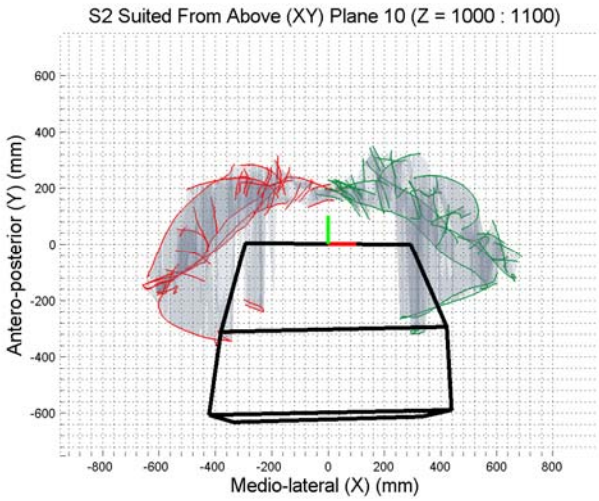

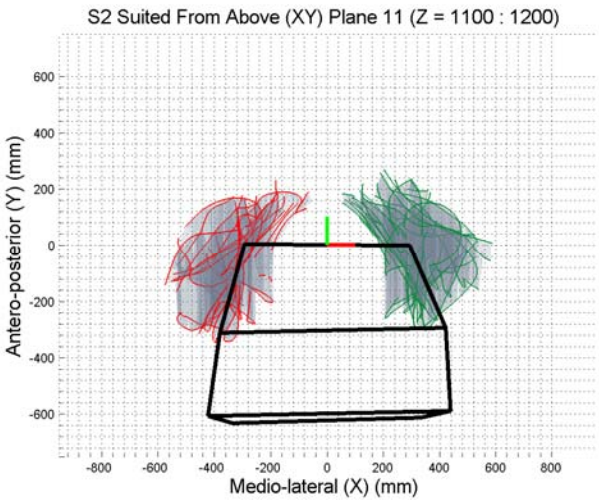

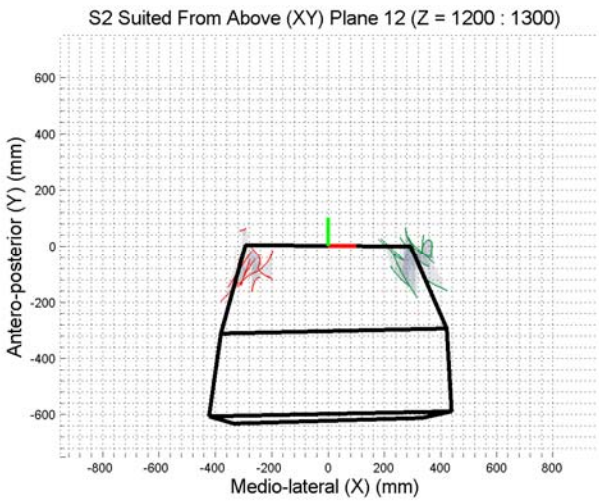

Unsuited

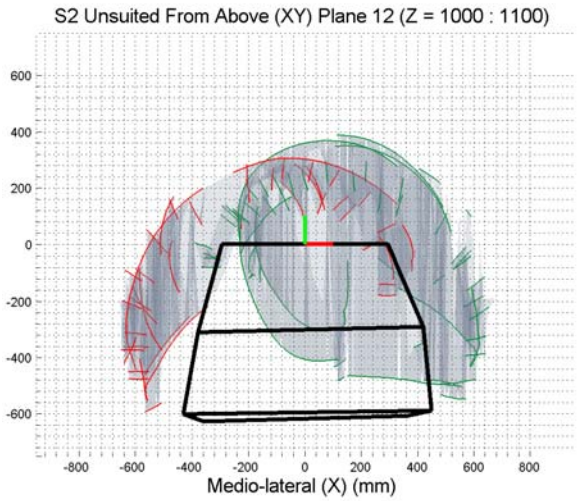

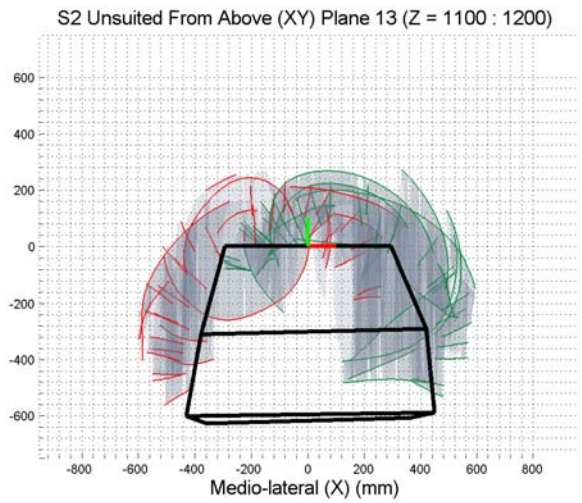

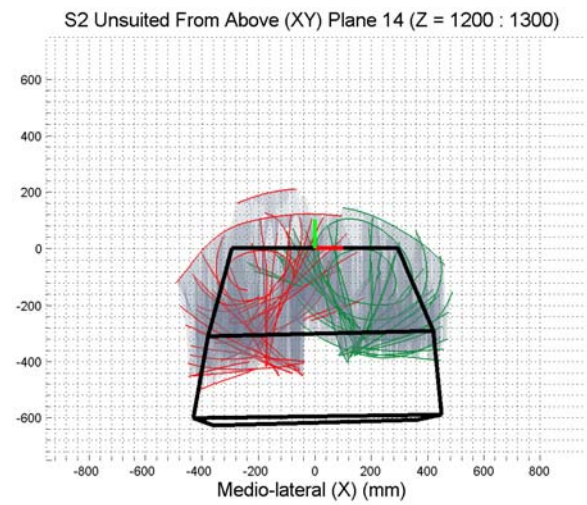

Suited

Unsuited

[No suited reach envelope within this plane]

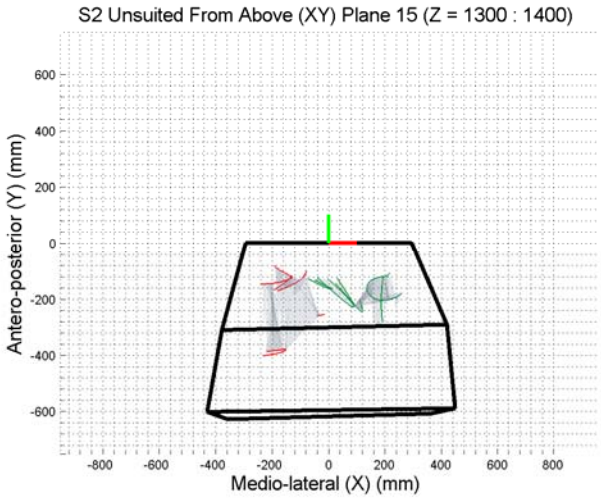

Figure 23. Triangulated reach envelope transverse plane cross-sectional slice data for Subject 2 suited and unsuited.

Suited

Unsuited

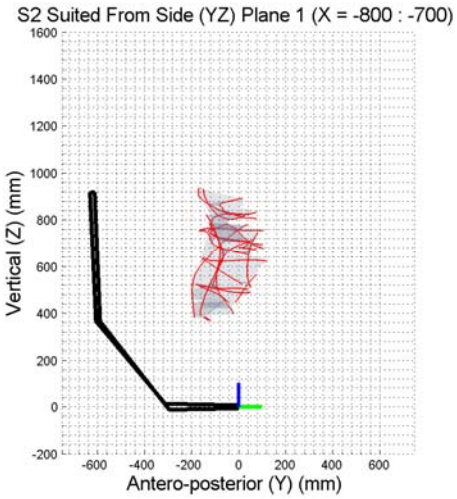

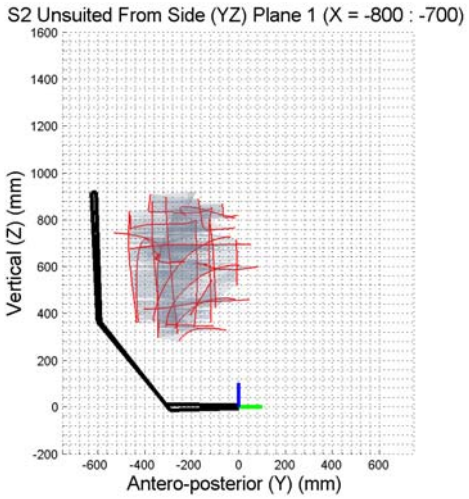

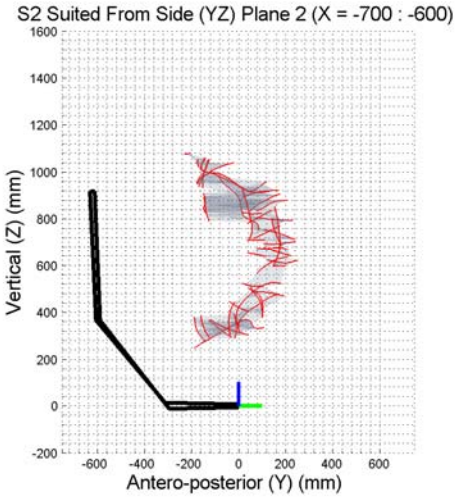

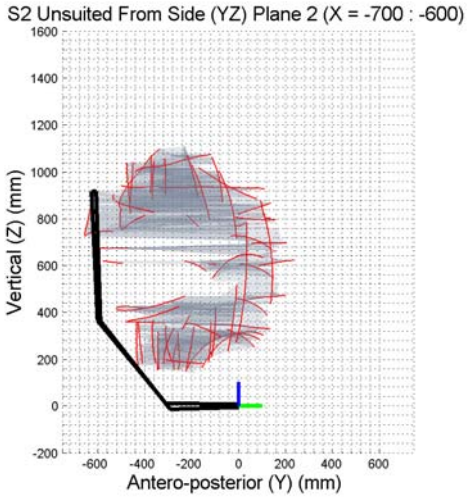

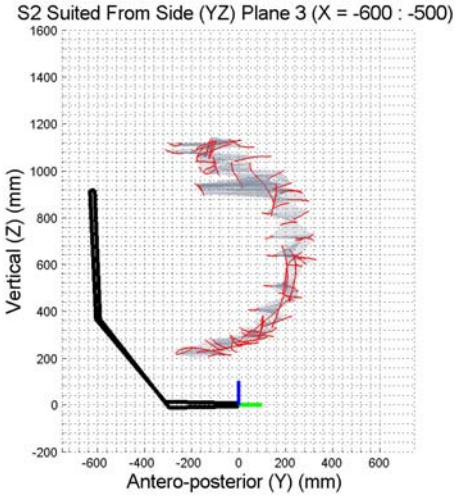

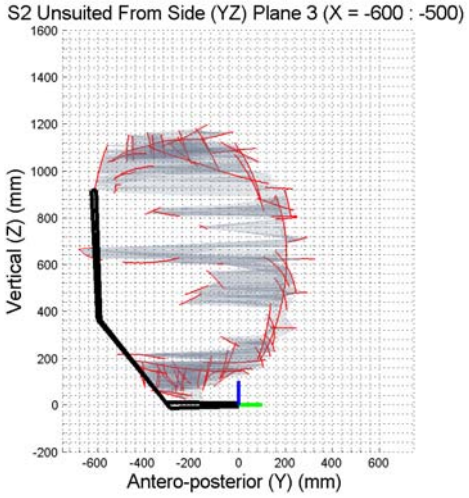

Suited

Unsuited

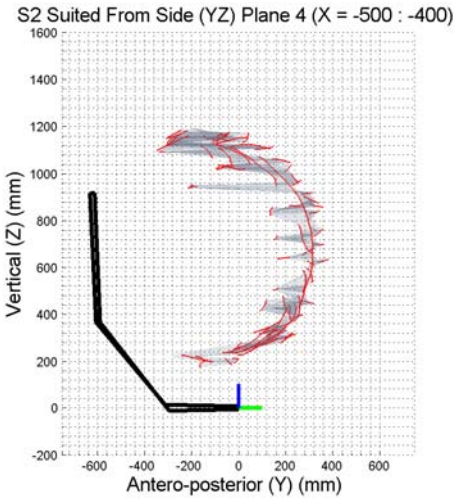

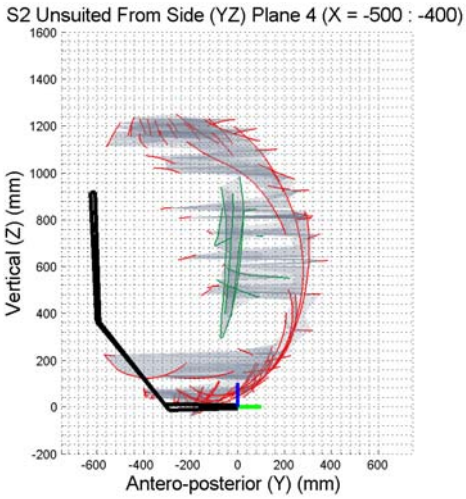

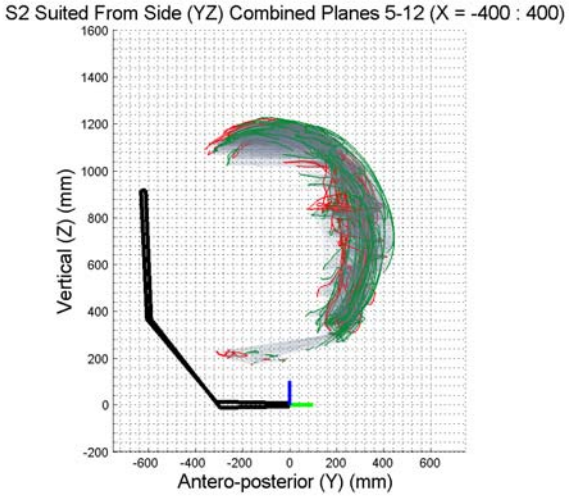

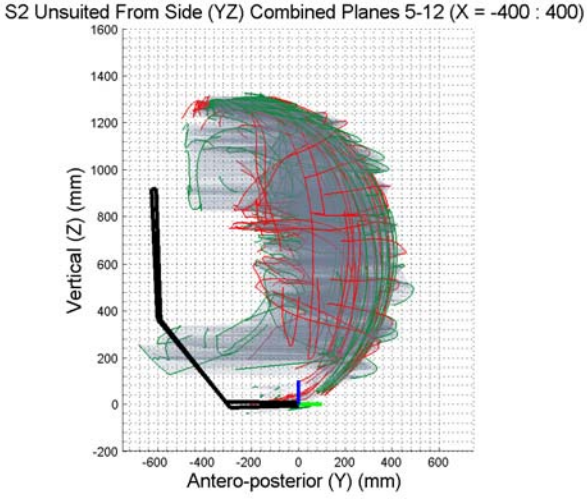

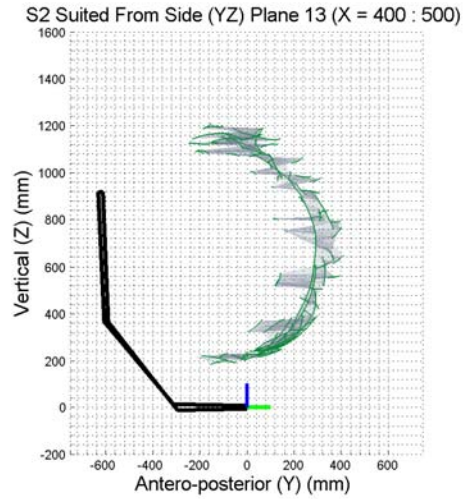

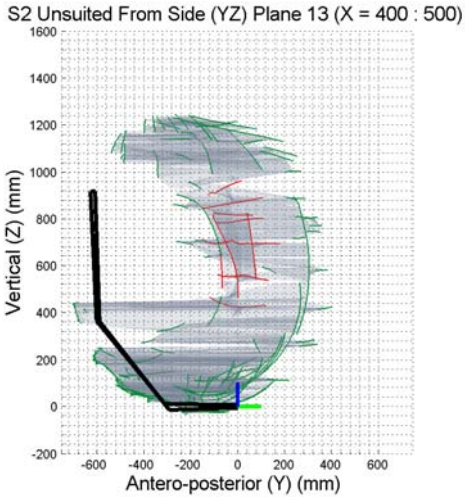

Suited Unsuited

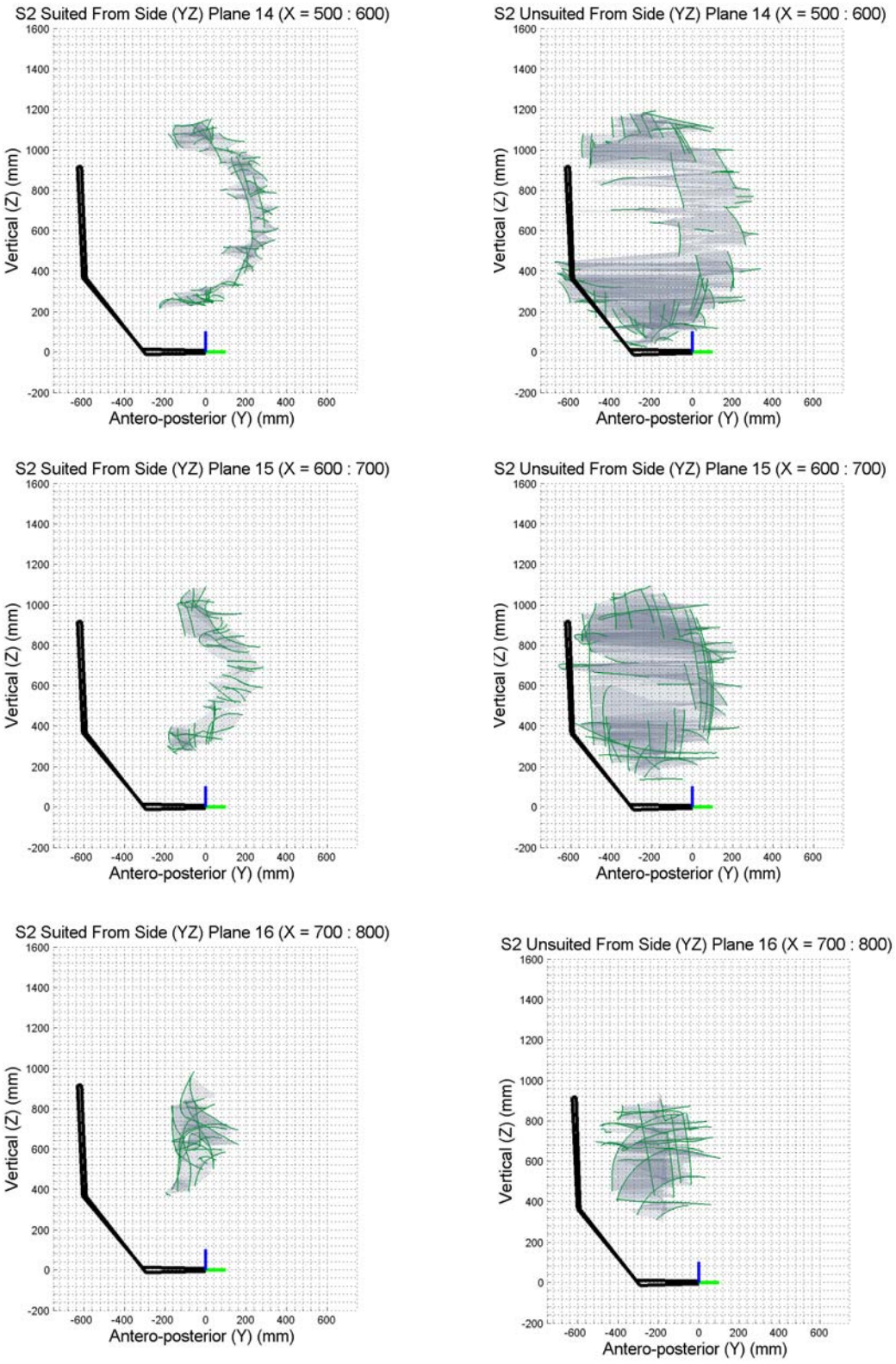

Figure 24. Triangulated reach envelope sagittal plane cross-sectional slice data for Subject 2 suited and unsuited.

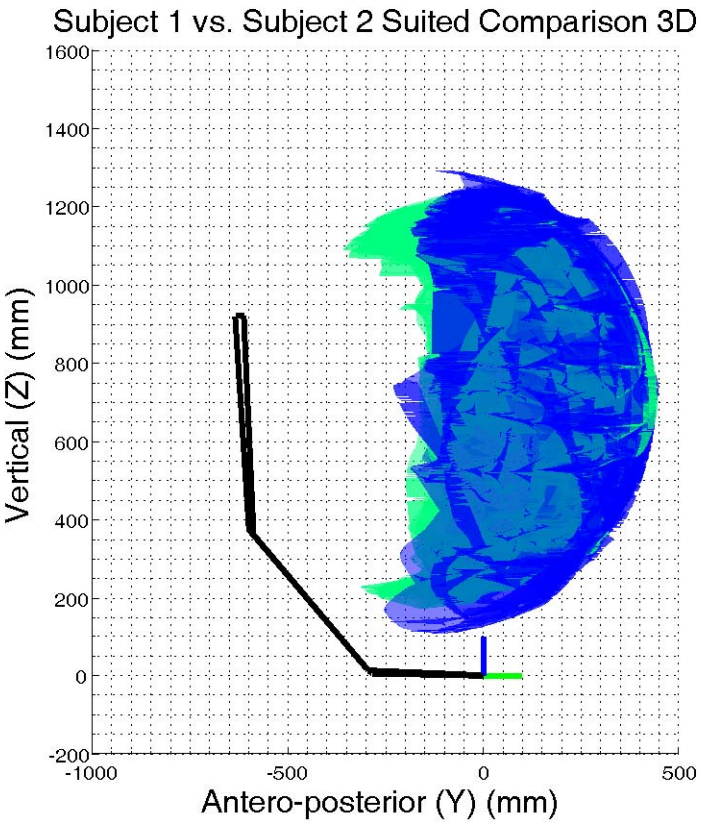
Subject 1 vs. Subject 2 Suited Comparison 3D
Vertical (Z) (mm)
Antero-posterior (Y) (mm)
1600
1400
1200
1000
800
600
400
200
0
-200
-1000
-500
0
500

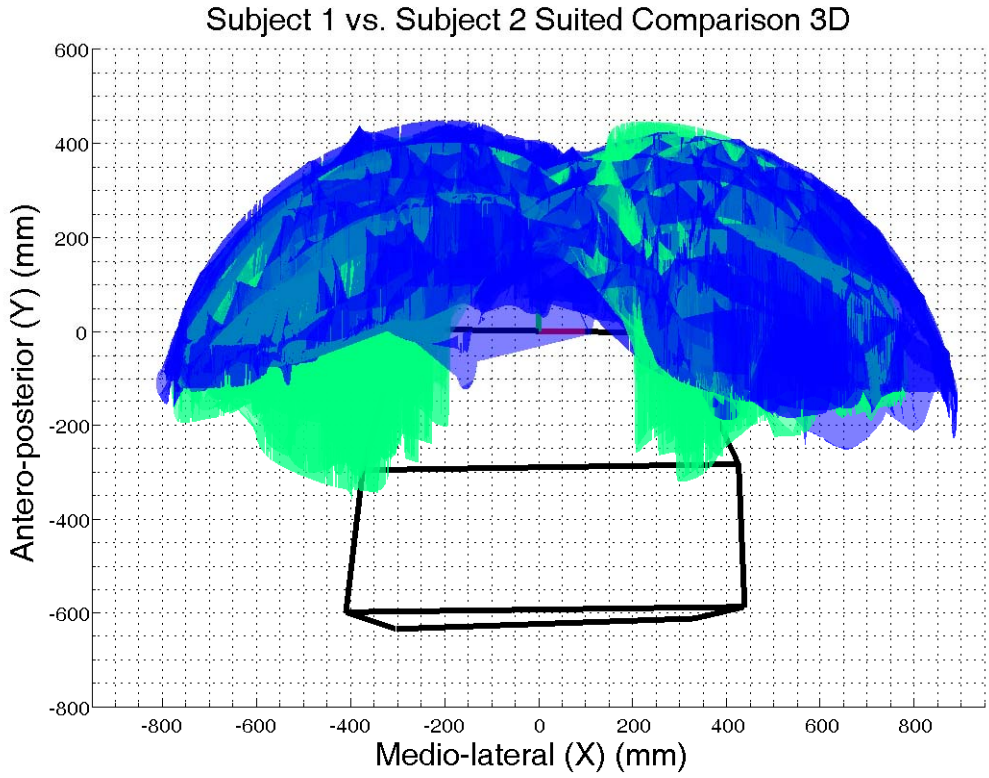
Subject 1 vs. Subject 2 Suited Comparison 3D
Antero-posterior (Y) (mm)
Medio-lateral (X) (mm)
600
400
200
0
-200
-400
-600
-800
-800
-600
-400
-200
0
200
400
600
800

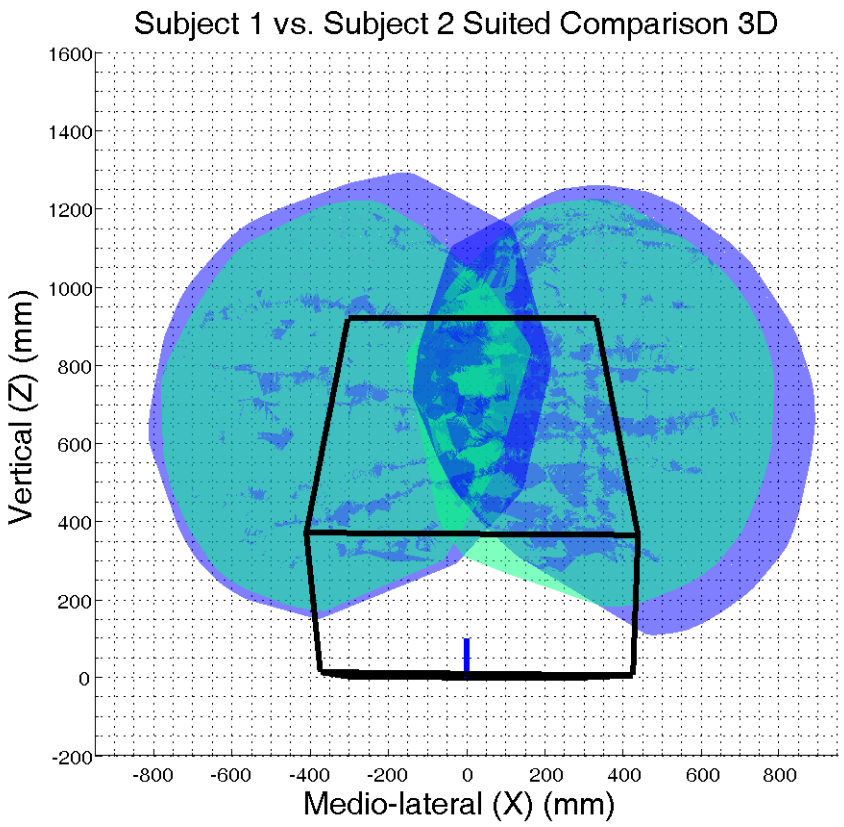

Figure 25. Comparison of suited reach envelopes for Subject 1 (Blue) and Subject 2 (Green).

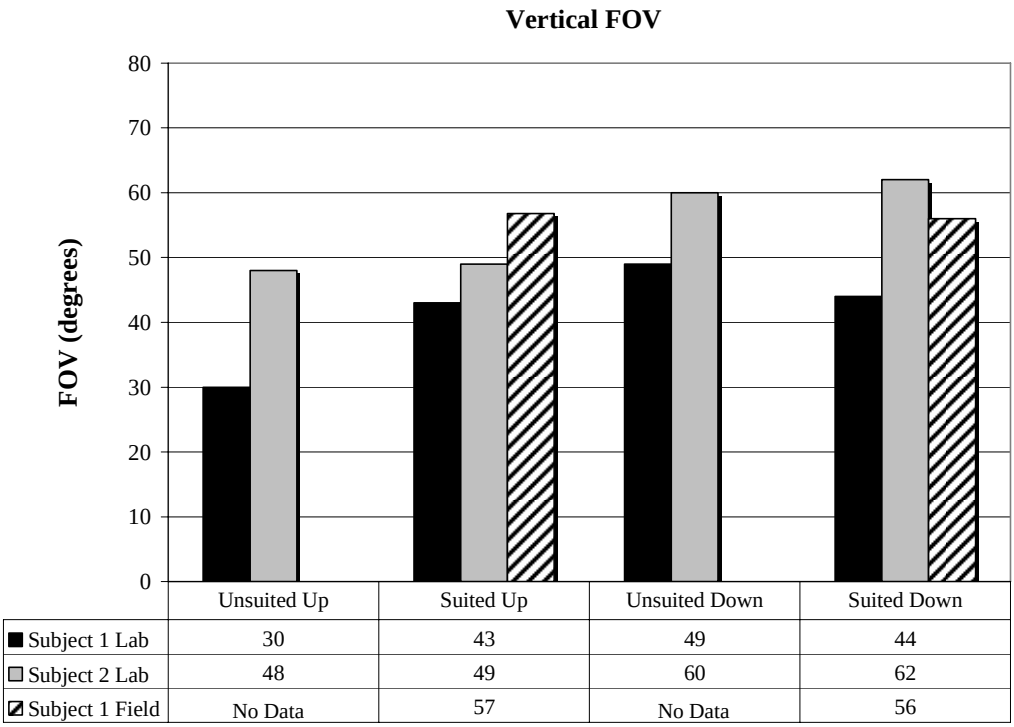

	Unsuited Up	Suited Up	Unsuited Down	Suited Down
Subject 1 Lab	30	43	49	44
Subject 2 Lab	48	49	60	62
Subject 1 Field	No Data	57	No Data	56

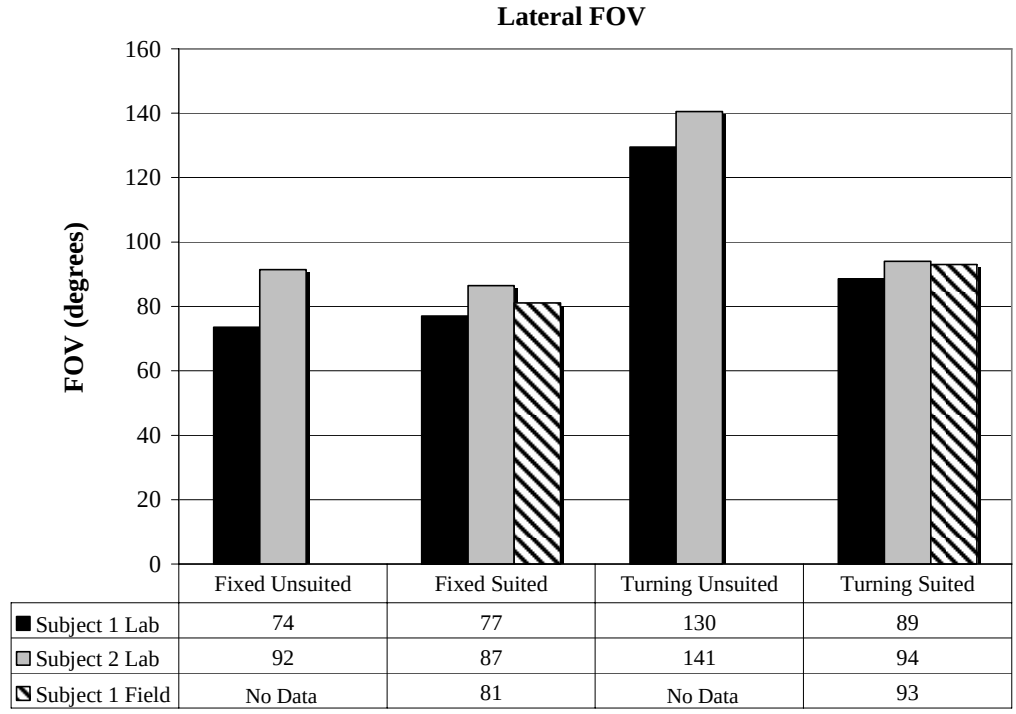

	Fixed Unsuited	Fixed Suited	Turning Unsuited	Turning Suited
Subject 1 Lab	74	77	130	89
Subject 2 Lab	92	87	141	94
Subject 1 Field	No Data	81	No Data	93

Figure 26. Field of Vision results for laboratory and field testing.

4. DISCUSSION

4.1 REACH ENVELOPE

Suited versus Unsuited Reach Envelopes
The comparison between suited and unsuited conditions allows a basic evaluation of the extent to which the Mark III suit restricts reach. As anticipated, the data indicate that the reach envelope is significantly affected by the Mark III suit as compared with unsuited conditions for both subjects. The extent to which subjects could move their torso during unsuited conditions was not strictly controlled; nonetheless, the comparison of reach envelope sizes between suited and unsuited conditions demonstrates that the suit restricts reach particularly in the vertical and posterior directions. Joint ranges of motion were not evaluated in this study, so the specific contributions of the suit elements to the reduction in reach envelope cannot be determined from this data.

The data collection and analysis protocol attempted to quantify both the outer and the inner bounds of the reach envelopes for the suited and unsuited conditions. The cross-sectional data provide quantitative verification that the suit affects the inner as well as the outer bounds of the reach envelopes; subjects were unable to reach as close to their own body while wearing the Mark III suit.

Movement of the torso inside the HUT
Interestingly, the maximum extent of lateral reach increased while wearing the suit, particularly in Subject 1 (Figure 19). The increase is likely because subjects were instructed to keep their torso stationary during the unsuited reach evaluation whereas during suited conditions subjects were free to move their bodies within the suit to the extent that they were able. Although the HUT itself did not visibly move during testing, it is likely that subjects were able to adjust their shoulder positions within the suit to facilitate marginally greater reach than during unsuited conditions. The same types of adjustments were also allowed during vertical and antero-posterior reach conditions, but the suit constrained the subjects such that maximal reach was attenuated in these directions.

Initial Torso Positioning
Both subjects were seated further back (posteriorly) in the seat during unsuited conditions than in suited conditions. Thus, relative to the seat, anterior reach was greater during suited than during unsuited conditions. When considering the overall range of reach in the A-P direction, the data confirm that unsuited reach is indeed greater than suited reach.

Laboratory versus Field Testing Suited Reach Envelopes
Comparison of the laboratory reach envelopes with the data points collected during the field data collection show some significant discrepancies (Figure 15, Figure 17, and Figure 21). All field testing data points are posterior to the corresponding reach envelopes as determined during laboratory testing. As discussed below, a combination of up to three possible factors may account for this result: a) different suit positions on the seat between field and laboratory testing, b) different subject positioning within suit, and/or c) measurement error associated with 2-D analysis in field testing.

Effect of Seat Type and Cushion Type

Different types of seats and seat cushions were used during laboratory and field testing. As Figure 27 shows, the seats and seat cushions used during laboratory testing and field testing were different and angle of the subject's upper body is noticeably different as a result.

The blue cushion shown in Figure 27 is of uniform thickness and was used during all laboratory testing. Conversely, the white seat cushion used during field data collection (Figure 27) is a wedge shape that is of greater thickness at the front of the seat than at the rear. The effect of the wedge cushion, possibly in conjunction with the different seat design, is to tilt the subject's upper body backward as the Figure shows.

The backward lean that is apparent during field testing but not laboratory testing affected the baseline position of the HUT, resulting in an inevitable posterior (and possibly downward) shift of the reach envelope.

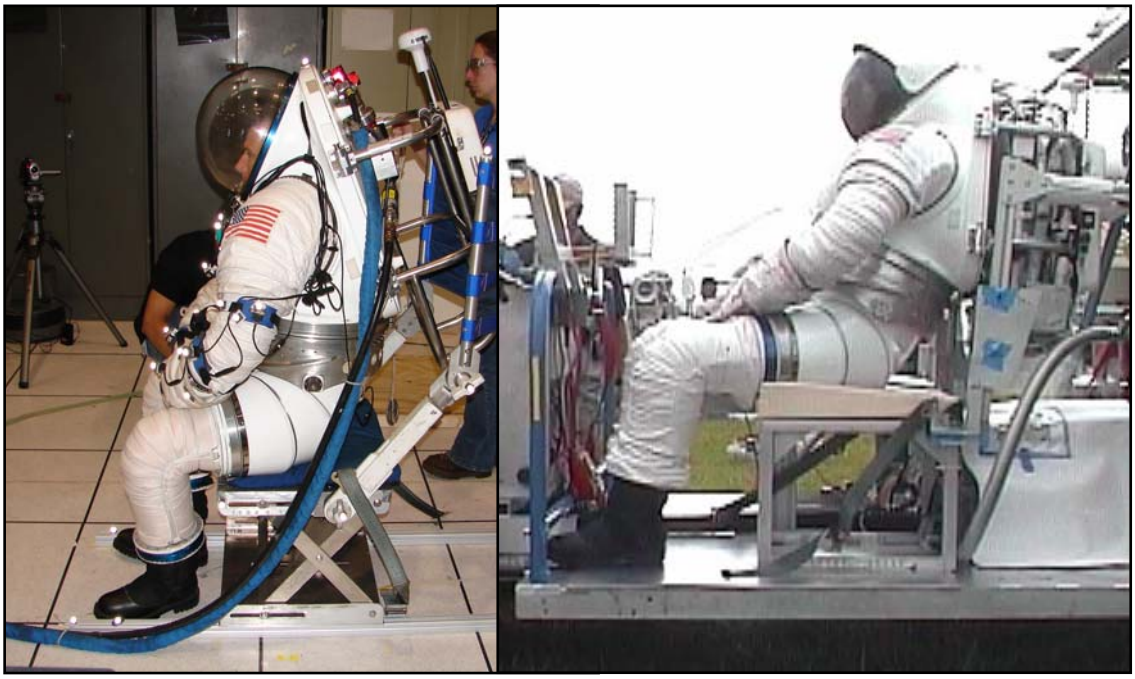

Figure 27. Comparison of seats, seat cushions, and posture between laboratory (left) and field (right) testing conditions.

Effect of Body Position within Suit

It is possible that the position of the subject within the suit also differed between laboratory and field testing conditions, contributing to the decreased anterior reach and increased posterior reach. If the subject's shoulder was positioned closer to the front of the suit during field testing, the allowable range of motion from the shoulder bearing would differ between conditions, causing a greater degree of posterior reach to be achieved at the expense of decreased anterior reach.

Effect of Measurement Error

As described in the Methods section, there are inherent limitations in 2-dimensional analysis of video footage. The accuracy associated with the analysis of field data in this study cannot be quantified but is known to be considerably less than the accuracy of the laboratory Vicon position data. It is possible that the discrepancies between laboratory and field position data are attributable in part to the errors associated with the 2-D determination of hand positions during the field testing.

Inter-Subject Differences in Suited Reach Envelopes

Because of the correlation between stature and other anthropometric parameters related to reach (such as arm length), the finding that vertical, lateral, and anterior suited reach ranges were slightly greater for the taller subject (Subject 1) was anticipated. The data indicate that Subject 2 was capable of slightly greater vertical and posterior reach immediately above the helmet (Figures 15-16) suggesting that Subject 2 may have had slightly greater upper-body strength and/or flexibility than Subject 1.

4.2 FIELD OF VISION

Comparison of 'turning' FOV while suited and unsuited indicates that the suit decreases lateral FOV from 130-141^{o} to 89-94^{o}. Results of the 'fixed' condition indicate that the suit has limited effect on peripheral vision when facing forwards with results varying between 74^{o} and 92^{o}. Field testing lateral FOV results were consistent with laboratory results.

The fixed vertical FOV was minimally affected by the suit in Subject 2. However, compared with unsuited laboratory conditions, the fixed vertical FOV of Subject 1 (up and down combined) increased by 8^{o} in suited laboratory testing and by 34^{o} in suited field testing. There is not a mechanism by which the suit could actually increase FOV. It follows that these observations must reflect large measurement errors, which are likely the result of unmeasurable head movement within the helmet affecting FOV measurements.

As described in Section 2, the measurement of FOV requires that the position of the eyes and the position of the object are known. The angle between these positions relative to some reference is then defined as FOV. If the position of the eyes actually moves forward or backward in the helmet relative to the initial measured position then the angle between the same object position and the eyes (i.e., the FOV) would increase or decrease, respectively. Thus, if the antero-posterior movement of the head within the helmet is not measured then the calculated vertical FOV will be inaccurate.

All four measures of FOV were greater during field testing than in the corresponding laboratory testing conditions. This may be a result of the subject's head being positioned farther forward in the helmet and thereby allowing a larger FOV.

The conclusions that can be drawn from the FOV data collected during laboratory testing are limited because of unmeasured movement of subjects' heads within the helmet. Asymmetries in FOV between left and right sides are presumed to be attributable to measurement error and/or asymmetry of the head position and orientation with respect to the suit helmet.

5. CONCLUSIONS AND FUTURE WORK

This report provides quantitative information on the reach envelope and FOV of two male subjects sitting in the SCOUT vehicle during suited (wearing the Mark III EVA suit) and unsuited conditions. Compared with unsuited conditions, medio-lateral reach was not significantly affected by the Mark III suit, whereas vertical and antero-posterior reach was significantly inhibited by the suit. Lateral FOV was reduced by approximately 40^{o} in the Mark III suit.

Differences consistent with the greater stature of Subject 1 were apparent between the reach envelopes of the two subjects. To generalize reach envelope sizes to other subjects, particularly those with different anthropometry, will require the collection of reach data from multiple subjects with a representative range of body sizes and particularly arm lengths.

The data reflected the intuitive fact that subjects' reach envelopes with respect to the rover are affected by their position upon the seat. Reach envelopes with respect to both the suit and the rover are also likely to be affected by the body's orientation with respect to the gravity vector. For example, anterior reach may be reduced when the rover ascends an incline. If future studies were to quantify the extent to which reach envelopes (relative to a suit reference system) are affected by body orientation, that data could be used to interpolate and extrapolate reach envelopes for any seat location, inclination, and cushion type.

The techniques employed in this study have not previously been used in the evaluation of reach envelopes. While the computer code developed for this project was refined following the data collection sessions, there were some limitations of the data that could not be overcome. In particular, it was evident that a larger number of data points are required to adequately determine the inner bounds of the reach envelopes. The inner bound represents the small volume immediately adjacent to the suit that the subject cannot reach because of the reduced ranges of motion allowed by the joints of the suit. In most instances, the outer reach bound rather than the inner bound will dictate the location of controls and connectors; indeed, the existing reach envelope data for EMU does not include any inner bounds (1). However, it is important that future reach envelope quantifications include accurate definitions of both inner and outer bounds in order to ensure that reach envelopes are not over-estimated. From the knowledge gained during this study, a more systematic data collection protocol has been developed, which is expected to produce more consistent and comprehensive quantification of the inner and outer bounds of the reach envelope.

The development of real-time data visualization will further enhance the quality and completeness of the data collected from each subject by identifying volumes that have been inadequately defined during the data collection protocol. Additionally, numerical approaches to reach envelope quantification are being investigated. A future application of the technique developed for this study is the validation of numerically derived reach envelopes. If the reach envelopes predicted by computer models are consistent with those measured using this technique computer models may represent a quick and accurate method by which to quantify suited reach envelopes for large populations of potential users.

Measurements of FOV used in this study were intended to provide approximations of vision angles under the different conditions. As discussed in Section 4, the inability to quantify head movements within the helmet introduced potentially large errors into the FOV measurements. Future studies should require that subjects are instructed not to move their heads within the helmet or alternatively employ a method by which to quantify the head movement.

In conclusion, the reach envelopes and fields of vision for two seated subjects were quantified while wearing the Mark III space suit. The data presented in this report may be utilized directly in the development of both the SCOUT vehicle cockpit layout, while the techniques are potentially applicable in the evaluation of other space suit reach envelopes and in the development of other human-machine interfaces such as spacecraft cockpits.

6. REFERENCES

1. "Space Shuttle System Payload Accommodations, NSTS 07700. Volume XIV, Revision K, Appendix 7: Extra Vehicular Activities," NASA 2000.

2. Schmidt, P.B., Newman, D.J., Hodgson, E., "Modeling Space Suit Mobility: Applications to Design and Operations," AIAA and SAE International Conference on Environmental Systems (ICES 2001), Orlando, FL, June 2001.

3. Barber, C.B., Dobkin, D. P., Huhdanpaa, H. T., "The quickhull algorithm for convex hulls," ACM Transactions of Mathematical Software, no. 22, pp. 469--483, 1996.

4. Bern, M., Eppstein, D. "Mesh generation and optimal triangulation." Tech. Rep. CSL-92-1, Xerox PARC, 1992. *Computing in Euclidean Geometry,* D.-Z. Du and F.K. Hwang, eds., World Scientific, 1992, pp. 23-90.

REPORT DOCUMENTATION PAGE

Form Approved
OMB No. 0704-0188

1. AGENCY USE ONLY *(Leave Blank)*	2. REPORT DATE	3. REPORT TYPE AND DATES COVERED
	November 2006	NASA Technical Paper

4. TITLE AND SUBTITLE
Reach Envelope and Field of Vision Quantification in Mark III Space Suit using Delaunay Triangulation

5. FUNDING NUMBERS

6. AUTHOR(S)
Andrew F. J. Abercromby, MEI Technologies, Inc.; Sherry S. Thaxton, Lockheed Martin; Elizabeth A. Onady, LZ Tech; Sudhakar L. Rajulue, NASA, Johnson Space Center

7. PERFORMING ORGANIZATION NAME(S) AND ADDRESS(ES)

Lyndon B. Johnson Space Center
Houston, Texas 77058

8. PERFORMING ORGANIZATION REPORT NUMBERS
S-987

9. SPONSORING/MONITORING AGENCY NAME(S) AND ADDRESS(ES)

National Aeronautics and Space Administration
Washington, DC 20546-0001

10. SPONSORING/MONITORING AGENCY REPORT NUMBER
TP-2006-213729

11. SUPPLEMENTARY NOTES

12a. DISTRIBUTION/AVAILABILITY STATEMENT

Available from the NASA Center for AeroSpace Information (CASI)
7121 Standard
Hanover, MD 21076-1320 Category: 39-08

12b. DISTRIBUTION CODE

13. ABSTRACT *(Maximum 200 words)*

The Science Crew Operations and Utility Testbed (SCOUT) project is focused on the development of a rover vehicle that can be utilized by two crewmembers during extra vehicular activities (EVAs) on the moon and Mars. The current SCOUT vehicle can transport two suited astronauts riding in open cockpit seats. Among the aspects currently being developed is the cockpit design and layout. This process includes the identification of possible locations for a socket to which a crewmember could connect a portable life support system (PLSS) for recharging power, air, and cooling while seated in the vehicle. The spaces in which controls and connectors may be situated within the vehicle are constrained by the reach and vision capabilities of the suited crewmembers. Accordingly, quantification of the volumes within which suited crewmembers can both see and reach relative to the vehicle represents important information during the design process.

14. SUBJECT TERMS	15. NUMBER OF PAGES	16. PRICE CODE
Weightlessness, weightlessness simulation, parabolic flight, zero gravity, aerospace medicine, astronaut performance, bioprocessing, space manufacturing.	58	

17. SECURITY CLASSIFICATION OF REPORT	18. SECURITY CLASSIFICATION OF THIS PAGE	19. SECURITY CLASSIFICATION OF ABSTRACT	20. LIMITATION OF ABSTRACT
Unclassified	Unclassified	Unclassified	Unlimited